Identifying post-translational modifications in vascular smooth muscle cell ageing and matrix stiffness response

Oliver Steward
100276251

Degree of Master of Science by Research, School of Chemistry, Pharmacy and Pharmacology, University of East Anglia

Date of submission
27/02/2025

14163 words

University of East Anglia | BIOMEDICAL RESEARCH CENTRE

University of East Anglia
SCHOOL OF PHARMACY

Contents **Page**

Acknowledgements

I would like to thank my primary supervisor Dr Derek Warren for all of the help and guidance he has provided me with during this project but also the time and effort he has put into this project to ensure it has been a success. I would also like to thank Finn Wostear, Alice Bradford and Reesha Solanki for their help in the lab with their assistance in training me in new techniques but also their help in running experiments successfully over the course of the year. I finally would like to thank Athina Smallwood for all her help in assisting the running for western blots and the help she provided during this project.

Abstract

We find ourselves in an increasingly ageing population and this has brought about an increase in the prevalence of age-related diseases. Cardiovascular disease (CVD) is the deadliest age-related disease in the world. The aorta is the largest artery in the body and carries oxygenated blood from the heart to the rest of the body. It changes shape in response to blood pressure to maintain a hydrostatic pressure reservoir and ensure there is enough pressure to move the blood around the entire body. This ability to change in shape is called compliance. Compliance is facilitated by the composition of the extracellular matrix (ECM), elastin provides the ability to stretch and recoil and collagen provides strength to prevent the aorta from over-stretching. However, as we age, the aorta undergoes ECM remodelling which increases aortic wall stiffness and reduces its compliance. Vascular smooth muscle cells (VSMCs) are the predominant cell type in the aortic wall, they sense increased aortic wall stiffness and further accelerate aortic dysfunction. Proteins are a critical component of all cell types, they are responsible for almost all cellular functions including regulating cell structure and support, metabolism, transport within cells and cell signalling. Proteins can be post-translationally modified (PTM), this is the process of chemical changes in the proteins that occur alter protein modification. This can result in changes to the protein structure and function.

This study aims to identify key post-translational modifications involved in both matrix stiffness response and ageing. This was achieved by growing VSMCs on 2, 12 and 72 kPa hydrogels to model matrix stiffness and using passage 8 versus passage 16 to model ageing. Additionally, to mimic ageing in cells an SiRNA knockdown of FACE1, which converts pre-lamin A into lamin A was carried out to mimic the pre-lamin A accumulation that occurs in ageing. Key genes upregulated in matrix stiffness response were chosen and validated in VSMCs, these genes were chosen as they were upregulated by matrix stiffness in a published bulk mRNA dataset of human aortic VSMCs. These were *NAT10*, *CHEK2, ANXA3* and *PDLIM1*. Western blot analysis of these genes in cultured human aortic VSMCs showed that there was a significant increase in NAT10 and PDLIM protein levels in response to increased stiffness. ANXa3 and Chk2 also trended towards upregulation in response to stiffness increases. NAT10 and Chk2 were also upregulated in aged VSMCs.

Microtubules can withstand the mechanical pressures exerted on the aorta and provide mechanical support to VSMCs. They are post-translationally modified to increase stability enhancing their ability to withstand pressure changes. Microtubules are made of an alpha and beta heterodimer, and these can be acetylated to increase stability. Total and acetylated alpha-tubulin were investigated in both 12 vs 72 kPa hydrogels to observe stiffness response changes and ageing through passage 8 vs passage 16 cells. There was no change in acetylation levels in stiffness response or ageing. Additionally, the microtubule stabilising protein Tau was investigated in mimicked ageing and there were no observed changes in Tau

phosphorylation levels. Finally, modifications of H3K9 were investigated. These were investigated due to their involvement in regulating inflammation-specific response genes which respond to MMPs that are involved in the remodelling of the ECM.

1. Introduction

1.1 Cardiovascular disease

Cardiovascular disease (CVD) is a group of deadly and prevalent diseases, being the second biggest cause of death in the UK. Due to the prevalence of CVD, it puts a strain on the health-care systems of the world. CVD is an umbrella term and encompasses several vascular-related diseases including coronary heart disease, peripheral arterial disease, stroke and vascular dementia. Coronary heart disease is the deadliest form of CVD, it is responsible for 11% of deaths in people under 75 in the UK. Most CVDs have common risk factors which include age, obesity, diabetes, hypertension and a genetic predisposition. Furthermore, lifestyle factors such as diet, alcohol intake and smoking play an important role in both the prevalence and prognosis of CVD in patients. Age is often identified as a major risk factor for developing CVD [1]. There are several treatments for CVD including the use of drugs including statins, beta-blockers and angiotensin-converting inhibitors. However, other approaches such as education on lifestyle choices and the impacts of smoking and dieting are often a more suitable approach to treating CVD.

1.2 The Aorta

The aorta is a critical component of the cardiovascular system, it is responsible for carrying oxygenated blood from the heart into the surrounding vasculature and organs. The aorta is comprised of 3 layers. The outermost layer is called the tunica adventitia, the middle layer is the tunica media, and the inner layer is the tunica intima. The tunica adventitia and media are the load-bearing layers of the aorta, the adventitia consist of layered collagen fibres to provide strength to the aorta [2]. The media is made up of vascular smooth muscle cells (VSMC), elastin, and collagen fibres. Finally, the tunica intima is the thinnest layer and is made of a single layer of endothelial cells [3]. Each layer of the aorta has an elastin lamina between to provide further elastic properties to the aorta, as shown in (**Figure 1**). The aorta can dilate and constrict in response to changes in blood pressure, VSMCs found in the tunica media of the aortic wall are mechanosensitive. This change in shape is done to maintain a hydrostatic pressure reservoir to ensure there is enough pressure to move the blood around the entire body [4]. This means that as blood pressure increases and the aortic wall stretches, the mechanosensitive VSMCs sense the increased pressure and contract to compensate [5]. Extracellular matrix (ECM) components such as elastin and collagen play a key role in healthy aortic function. Elastin enables the aorta to stretch and recoil through the cardiac cycle. Blood pressure increases in the aorta are caused by the heart.

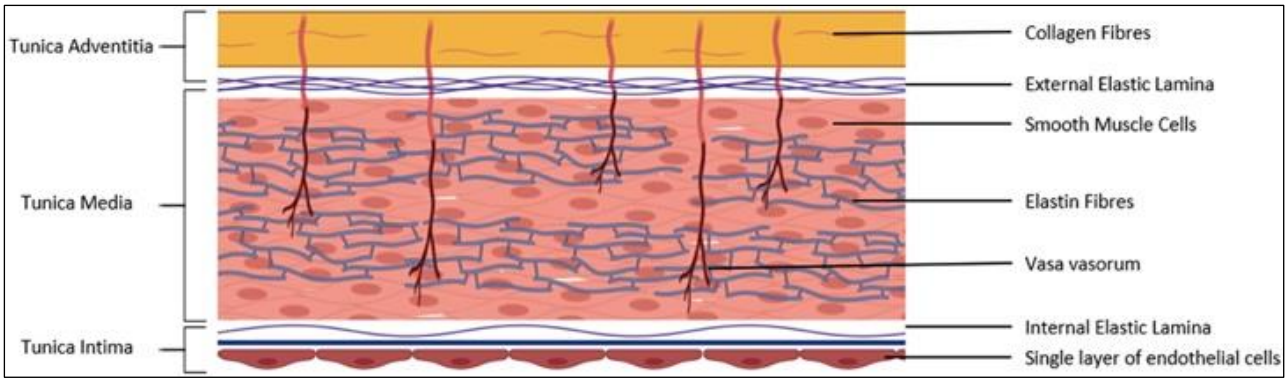

Figure 1.

The 3 main layers and components of each layer of the aortic wall. The outer tunica adventitia, containing the majority of the aorta's collagen content. The middle tunica media is the largest layer of the aorta, it is separated from the adventitia by a layer of elastic lamina. The media is constituted of smooth muscle cells, elastin fibres and the vasa vasorum which provides blood and nutrients to the SMCs. Finally, the tunica intima is the inner most layer of the aorta and contains an elastic lamina and a single layer of endothelia cells.

(Figure sourced from;[6]).

As the aorta dilates in response to blood pressure increase, caused by ventricular systole, this forces blood into the aorta and causes a temporary increase in aortic hydrostatic pressure. The elastin extends and the VSMCs relax to change the shape of the aorta and increase the size of the lumen to compensate for the pressure increase (**Figure 2**). Then during diastole, the elastin recoils and VSMCs contact to return the aorta to its resting state shape forcing the blood through the aorta and into the surrounding vasculature, allowing continued blood flow through the aorta [7]. This process is a continued pulsative flow of blood as is often referred to as the Windkessel function.

Collagen is present in the aortic wall to provide strength between cells and to allow the aorta to withstand pressure increases. Collagen provides mechanical strength and structure but also tensile strength and stiffness [8]. The ability of the aorta to change shape in response to blood pressure is called compliance, and it is an essential process in the body.

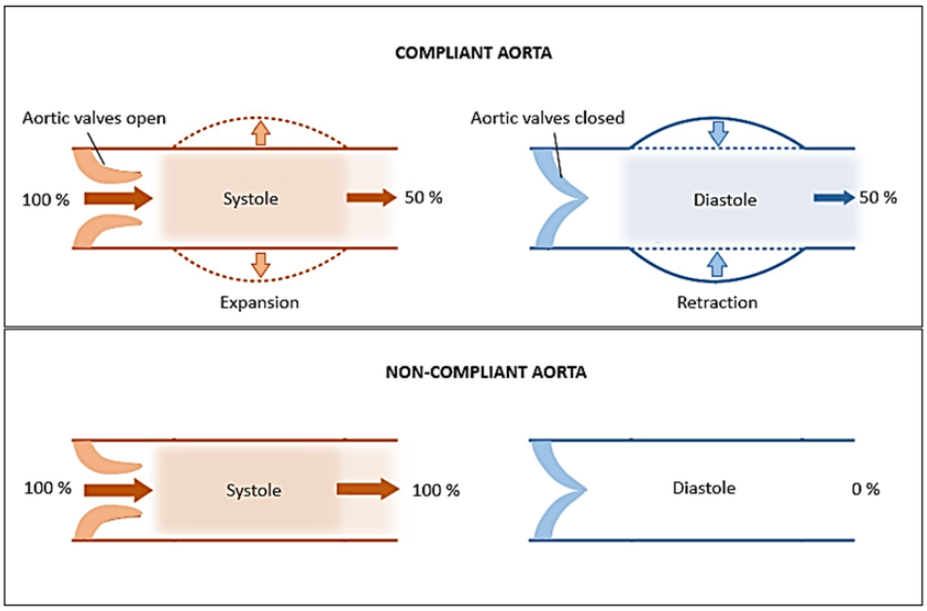

Figure 2.

Aortic compliance is the ability of the aorta to change shape in response to blood pressure increases caused by ventricular diastole. As the aortic valves open, blood rushes in and the aorta expands in diameter to allow the blood to enter, this is aortic systole. It then recoils forcing the blood to rush out of the aorta into the peripheral vasculature returning to its original shape, this is diastole. However, in a non-compliant aorta, there is no change in shape during systole or diastole in the aorta.

(Figure sourced from;[9]).

Without the function to change shape and increased lumen size, the increases in pressure would be potentially damaging to the aortic wall and could lead to aortic dissection. However, due to the high levels of elastin which allow the aorta to stretch and collagen for strength, the aorta is able to expand to allow blood to enter the aorta and reduce the hydrostatic pressure and then recoil to expel the blood further through the vasculature [10].

1.3 Arterial stiffening

During ageing, many processes occur which affect the compliance of the aorta, this process is known as arterial stiffening. One of the major risk factors that arise from ageing is the degradation of elastin in the aortic wall. Matrix metalloprotease (MMP) expression increases with age. Specifically, MMP-2, MMP-3, MMP-7, MMP-9 and MMP-12 are known to degrade elastin and its pre-cursor tropoelastin. MMPs cleave specific sites in elastin causing the fibres to fragment and become non-functional [(11)]. Expression of Tissue inhibitors of MMPs (TIMPs) is also reduced during ageing, this prevents them from binding to and inhibiting MMPs, thus aiding in elastin degradation [12]. Collagen remodelling occurs during ageing, in a healthy aorta, collagen is thin, wavy and sporadic in arrangement. However, during ageing, the collagen fibres, become thick and linear in arrangement [13] . The change in collagen structure, in addition to increased elastin degradation, can result in the aortic wall becoming stiffer and less compliant [14]. Collagen crosslinking increases with age, this occurs through the increased production of key amino acids required for crosslinking which include histidinoalanine, pentosidine, isodesmosine and pyridinoline [15]. Crosslinking also can be caused by the accumulation of produced by glycation and oxidation of sugars and amino groups. Both of these cause bridges to form between collagen fibres and crosslinks to form [16]. The increase in collagen content and crosslinking between fibres increases the stiffness of the aorta and contributes to the risk of age-related diseases.

These changes often occur through post-translational modification (PTM) of key proteins and components of the aorta, these modifications can include acetylation, phosphorylation, methylation and more. Within the aorta, PTMs can occur in the microtubules, elastin, collagen type I and many more key components [17]. Furthermore, as the aorta ages the three tunica layers thicken, most significantly the tunica intima thickens and becomes load-bearing. This is often associated with atherosclerosis.

All of these factors contribute to the reduction in compliance of the aorta, inhibiting the ability to change shape as effectively in response to changes in pressure, resulting in increased stress on the aorta and increased risk of cardiac events [18].

1.4 Vascular Smooth Muscle cell function and phenotype

Vascular smooth muscle cells (VSMC) are a highly contractile cell type found in a quiescent state in the healthy aortic wall. VSMCs are found in a healthy contractile (differentiated) or a diseased synthetic (dedifferentiated) phenotype [19] (**Figure 3**). Contractile phenotype VSMCs have highly contractile properties and reduced proliferative and migrative activity in these cells. Whereas synthetic VSMCs are hypertrophic, highly proliferative and migratory [20]. VSMCs exhibit their highly contractile function due to the expression of key genes including calponin (CNN1), smooth muscle myosin heavy chain and smooth muscle actin [21]. Actin and myosin in the VSMCs interact to generate actomyosin forces in the cells.

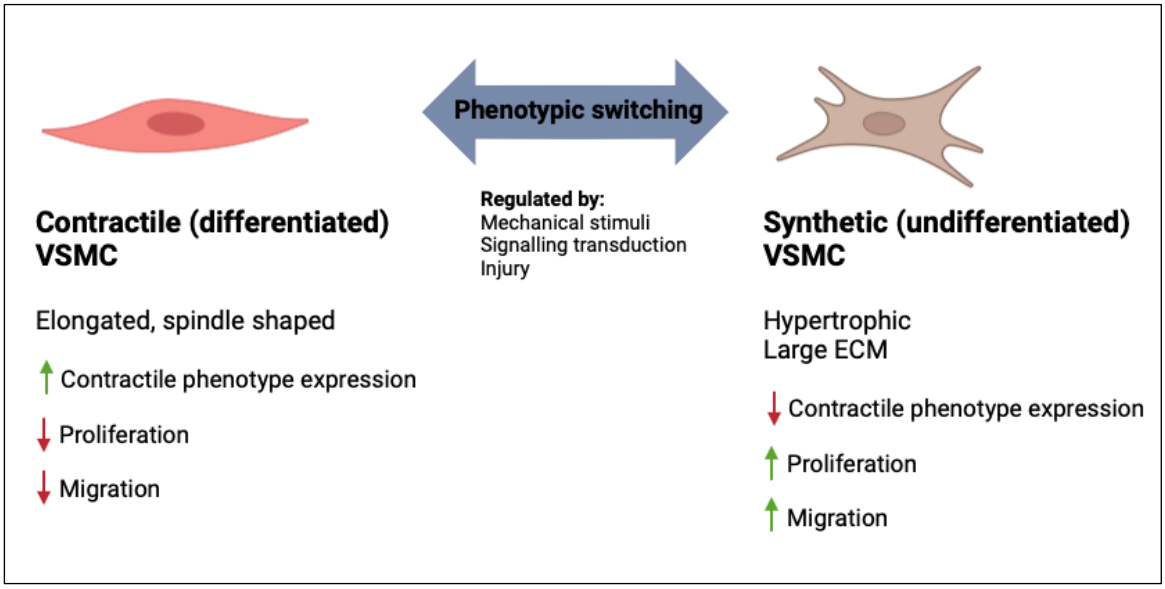

Figure 3.
VSMCs undergo phenotypic switching in response to various stimuli. When active VSMCs differentiate into a contractile phenotype and de-differentiate into a synthetic phenotype when inactive.
(Figure generated in Biorender.com)

VSMCs are mechanosensitive cells and can detect changes such as pressure, stretch and force [22]. This is important for regulating the diameter of the aorta's lumen, VSMCs can contract and relax to aid in the process of dilation and constriction of the lumen in direct response to the blood pressure changes [23]. Furthermore, VSMCs can maintain the vascular tone of the aorta, through the generation of actomyosin-derived forces to regulate the contractile activity of the aorta [24]. Actomyosin-derived forces are generated from the interactions of α-smooth muscle actin (αSMA) and smooth muscle-myosin heavy chain (SM-MyHC). These interactions

cause cells to contract [25]. In the contractile phenotype, VSMCs have more αSMA and SM-MyHC present, this enhances actomyosin interactions.

Both contractile and synthetic VSMC phenotypes can generate actomyosin force via stimulating interactions between myosin II and filamentous actin. This is regulated in both phenotypes by factors including angiotensin II, that bind to receptors on the VSMC surface to induce contraction [26]. Increased Matrix rigidity activates Rho/ROCK signalling inducing actin polymerisation and myosin light chain phosphorylation by Rho-associated coiled-coil kinase (ROCK). This results in increased actomyosin interaction and cell contraction resulting in further matrix stiffening [27]. Ca2+ binds to troponin-C on the actin filaments causing a conformational change in troponin structure resulting in tropomyosin strands to shift revealing the sub-domain 1 site of actin to be exposed allowing myosin heads to bind inducing the contractile cycle to start [28]. Ca2+ and calmodulin-dependent myosin light chain kinase phosphorylate myosin light chains at the myosin-binding subunit (MYPT1). MYPT1 is phosphorylated at several sites by ROCK which inhibits phosphatase activity, this promotes the contractile activity [29].

During ageing, changes to matrix rigidity and blood pressure caused by ECM remodelling result in enhanced actomyosin-derived force generation and increased cell contraction, this contributes to a further increase in matrix rigidity [30]. As the aorta ages, actomyosin force generation is increased and VSMCs contract which contributes to the overall reduction in aortic compliance and increased wall rigidity associated with age.

PDLIM1 is a cytoskeleton-associated protein involved in regulating the organisation of the actin cytoskeleton through the assembly and disassembly of actin stress fibres. Stress fibres allow for increased contractibility in VSMCs, PDLIM1 localises to actin stress fibres and acts as an adaptor molecule to recruit signal molecules to the fibre. Additionally, the inhibition of PDLIM1 results in a reduction of the formation of stress fibres [31].

VSMCs are also known to synthesize elastin, fibronectin and collagen type I, III and IV used to increase the elasticity, strength and compliance of the aorta [32]. Healthy VSMCs are found in the contractile phenotype, which means they can regulate the shape and size of the lumen in response to blood pressure changes. Contractile VSMCs can be identified by expression of the protein markers, smoothelin and smooth muscle-myosin heavy chain (SM-MHC) [33]. Smoothelin interacts with actin filaments and SM-MHC interacts with contractile filaments to regulate VSMC contractility [30]. However, in the synthetic phenotype, cells are unable to regulate lumen size and the ECM is remodelled and stiffer. This comes from an increase in collagen build up and a reduction in elastin (**figure 3**).

1.5 VSMC mechanotransduction

Mechanotransduction is the process of VSMCs sensing and converting mechanical stimuli into a biochemical response resulting in contractile movement of the cells [34]. Mechanical stimuli can include matrix stiffness, shear stress, and transmural and pulsatile pressure. VSMCs can mechanosense in several ways, one main way is through various ECM components [35].
The mechanotransduction pathway, transfers mechanical stimuli from the outside of the cell through the ECM, to the cell nucleus eliciting gene expression. Stimuli exerted onto the ECM are transmitted to the cytoskeleton across the cell membrane through adhesion molecules including integrins, Cadherins and G-protein coupled receptors (GPCRs). Signalling pathways transmit the signal to the nucleus through LINC complexes where it enters the nucleus through nuclear pores in the nuclear lamina where it interacts with chromatin to regulate gene expression.

Lamin A and C are proteins found in the nuclear lamina which are responsible for critical cellular processes including maintaining the cell's structural stability, chromosomal organisation, cell motility, gene regulation, DNA damage repair, cell differentiation and mechanosensing [36]. Lamin regulates these processes through musculoskeletal-cytoskeletal interactions [37], lamin A and C form a meshwork in the nucleus that regular mechanical properties through ECM, cytoskeleton and focal adhesion interactions [36]. In response to increased matrix stiffness and mechanical stimuli lamin A is known to also increase, the increase in lamin also increases in the lamin meshwork in the nucleus which further contributes to increased stiffness [38]. Lamin A/C are known to be mechanoresponsive proteins, they respond to changes in ECM stiffness. Mechanical stimuli exerted on the cell surface are transmitted to integrins which connect to the nuclear lamina through the LINC complex [39]. The LINC complex links the cytoskeleton to the nucleoskeleton through nesprin and sun proteins (**Figure 4**). Lamin A in the nuclear lamina, lamin A transmits the signal to the nucleus to activate gene transcription. There are several ways lamin A interacts with the nucleus, it can directly interact with the nucleus to transmit the signal [40] or it can interact with other proteins which interact with the nuclear membrane like emerin, lamina associated polypeptide 2 [41]. Mutations to the gene encoding lamin A/C (LMNA) have been seen to result in the formation of a group of pathologies called laminopathies. These laminopathies can increase the development of progeria, atherosclerosis and increase the incidence of stroke and heart attacks [42].

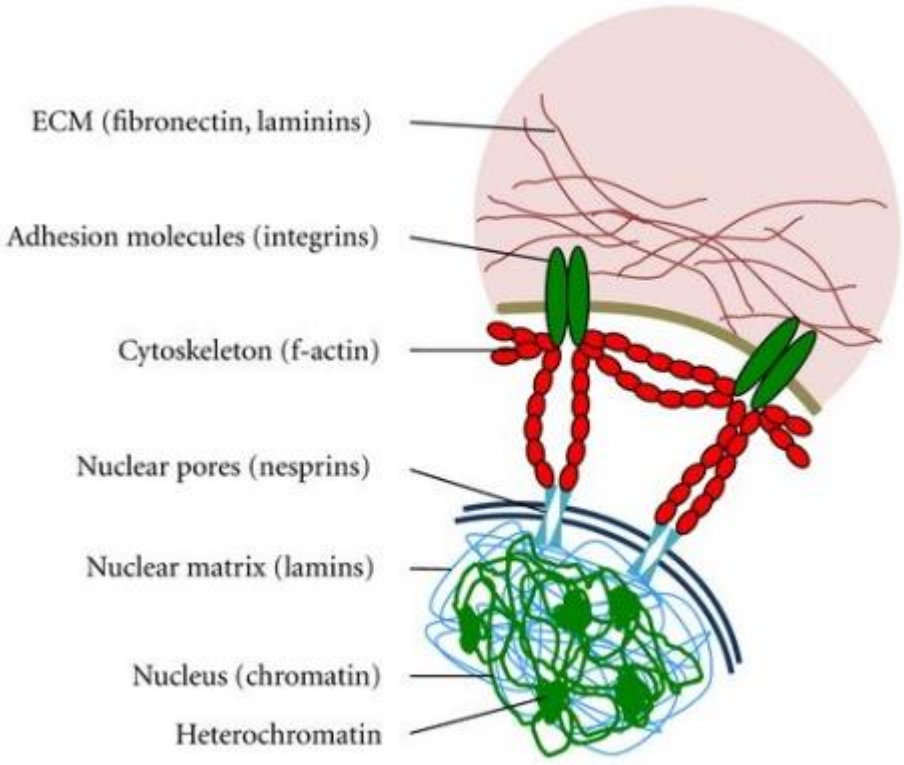

Figure 4.

Mechanotransduction pathway linking mechanical stimuli exerted on the ECM to the cytoskeleton through integrins an adhesion molecule. The cytoskeleton links to the nuclear envelop through LINC complexes where the signal is transmitted to the nucleus to regulate gene expression.

(Figure sourced from;[43]).

Pre-lamin A is converted to mature lamin A by the proteolytic cleavage of Pre-lamin A by one of two processing enzymes called farnesylated proteins-converting enzyme 1 (FACE1) or zinc metallo-endoprotease (Zmpste24) [44]. Pre-lamin A is the precursor of Lamin A and is known to accumulate in ageing and prevents the conversion into Lamin A. Pre-lamin A accumulation is also seen in many cardiovascular diseases ranging from atherosclerosis to cardiomyopathy. Accumulation of pre-lamin A in proliferative VSMCs is known to reduce DNA-damage repair and induces DNA-damage signalling that drives VSMCs into premature senescence [45]. This process is driven by alterations to the nuclear lamina function caused by accumulation of pre-lamin A and reduction in mature lamin A. Rac1 is a GTPase that is known to regulate microtubule stability in the VSMC cytoskeleton but also regulate VSMC migration. Prelamin A accumulation is known to reduce Rac1 activity in cells, Rac1 increases microtubule stability in cells through the activation of p21-activated kinase (PAK) which phosphorylates and inactivates a microtubule destabilising protein called stathmin at its serine 16 residue which results in increased microtubule stability [46]. In migration Rac1 is known to regulate and reduce

VMSC migration, the accumulation of prelamin A reduces Rac1 and prevents it from diminishing migrational activity. Therefore, a loss in mature lamin A and build-up of prelamin A could suggest that due to changes in cellular function, reduction in Rac1 activity and a reduction/loss of key functions in VSMCs including mechanosensing and signal transduction.

Integrins can connect the ECM to actin filaments at the focal adhesion complex in the β-subunit of the integrin. Integrins interact with proteins such as FAK, vinculin, paxillin and talin to form focal adhesion complexes. These complexes allow signalling pathways such as MAPK and Rho GTPase to activate starting a cascade of biochemical signalling [47]. This allows for signal transduction in an outside-in direction.

The FAK-PIK3 signalling pathway interacts with integrin β1 and β3 in the cell membrane to regulate VSMC proliferation and migration through the FAK-dependent Yes-associated protein 1 (YAP1) pathway [48]. Integrin $\alpha_v\beta_3$ regulates phosphorylation of FAK resulting in YAP dephosphorylation leading to increased proliferation and migration. YAP1 is involved in actin-cytoskeleton mechanical signalling by mechanosensing changes in ECM stiffness [49] and focal adhesions, this results in increased YAP localisation to the nucleus. YAP binds to transcription enhancer-associated domain 1–4 transcription factors (TEAD1–4) to activate downstream gene expression, resulting in an increase in VSMC proliferation and migration [50]. Integrins can play a major role in the progression of many types of CVD, mainly in atherosclerosis lipid fats interact with integrins both in the endothelial cells in the tunica intima but also in the VSMCs in the tunica media [51]. In endothelial cells, integrins interact with fats to promote endothelial inflammation through several different pathways including JNK and NF-kB signalling [52]. Endothelial inflammation is known to result in plaque formation and intimal thickening. In VSMCs, integrin α5β1 interacts with Milk fat globules-epidermal growth factor 8 (MFG-E8) to activate TGF-β signalling and promote MMP2 expression to result in VSMC calcification [53]. integrin α5β3 interacts with thrombin to increase VSMC proliferation and migration through phenotypic switching to lead to VSMC cell growth and vascular wall thickening [54].

Another pathway of signal transduction is through cadherin and GAP junctions, these occur at cell-cell interaction points in the aortic wall where VSMCs adhere to one another. Cadherins are calcium-dependent transmembrane receptors and bind VSMCs together through catenin-actin filament interactions [55]. Cadherins transduce mechanical stimuli across the cell membrane and activate Wnt and β-catenin signalling to regulate gene expression in response (**Figure 5**) [56].

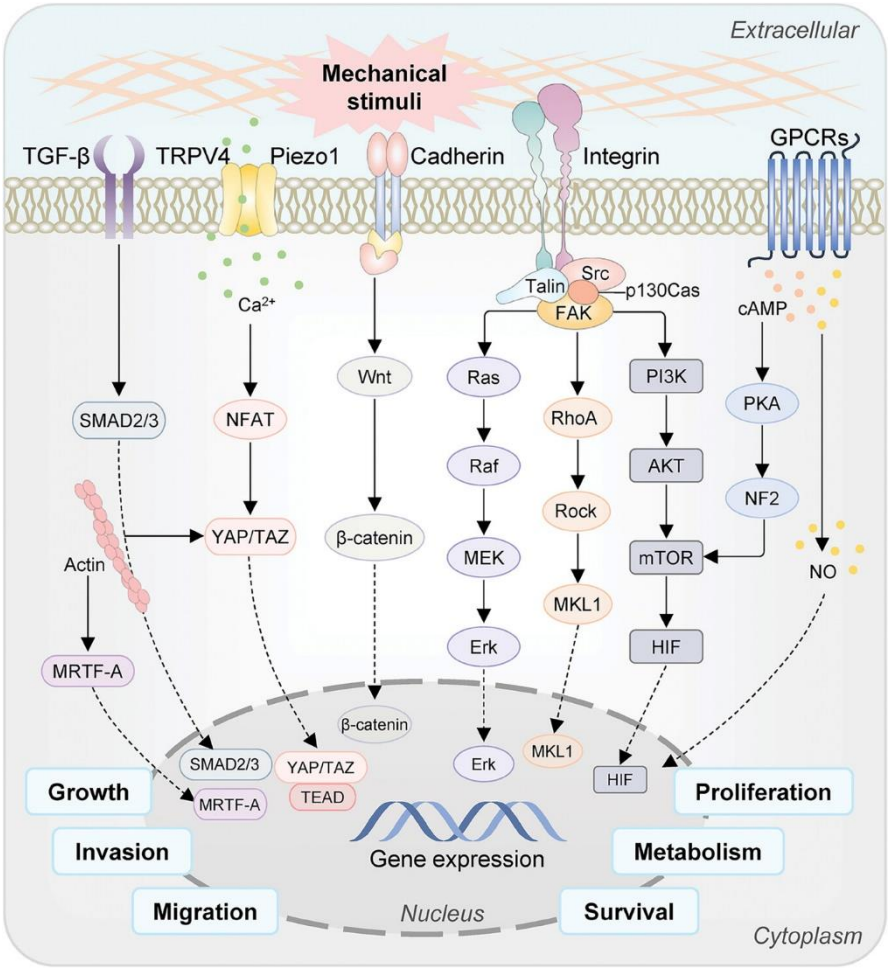

Figure 5.

Schematic showing the major signalling pathways involved in mechanotransduction in cells. Membrane bound channels serve as adhesion molecules to allow signal transmission into the cell. Different adhesion molecules activate different signalling pathways resulting in gene transcription changes.

(Figure sourced from;[56])

Actin, intermediate filaments, and microtubules are the 3 components of the cytoskeleton found in VSMCs and all play a role in signal transduction. Actin is the most abundant cytoskeletal in VSMCs and comes in 4 subtypes; α-smooth muscle actin (SMA), β-non-muscle actin, γ-SMA, and γ-cytoplasmic actin [57]. It interacts with TGF-β receptors to propagate TGF-β signalling which results in cell differentiation and proliferation [58]. Intermediate filaments form dense bodies which have dense plaques in the cytoplasm, allowing the propagation of mechanical signals to pass through the cell membrane [59]. Microtubules are believed to mediate Ca^{2+} signal transduction in cells, the literature surrounding this suggests microtubules either regulate calcium-independent or calcium-dependent contraction in cells or alternatively it is believed they regulate both [34]. All 3 of these components are crucial to interacting with LINC complexes to connect the cytoskeleton to the nucleoskeleton.

Additionally, there are many mechanosensitive ion channels in VSMCs that are involved in mechanotransduction, Piezo1, MscS, MscL, TREK and two-pore domain K+ channels (K2P) are known mechanosensitive ion channels in VSMCs [60]. These ion channels work via lipid bilayer tension in a process called the force-from-lipid (FFL) (**figure 6**). This process results from the push-pull forces created from phospholipid head and acyl tail interactions in the bilayer then transfers force from the lipids to the proteins in the membrane to pull the ion channels open [61]. This allows ions to enter the channels and transfer across the membrane, allowing signal transduction. In response to mechanical stimuli, VSMCs are known to release transforming growth factor β (TGFβ) and vascular endothelial growth factor, alongside regulating angiotensin II receptors [62]. GAP junctions are another Ca^{2+} membrane-spanning channel that allows signal transduction through Ca2+ ions and the downstream activation of the ERK-MAPK pathway resulting in changes to gene expression as a result [63]. These responses allow VSMCs to respond to the stimuli in several ways including cell contraction, secretion, cell growth and cell division [64].

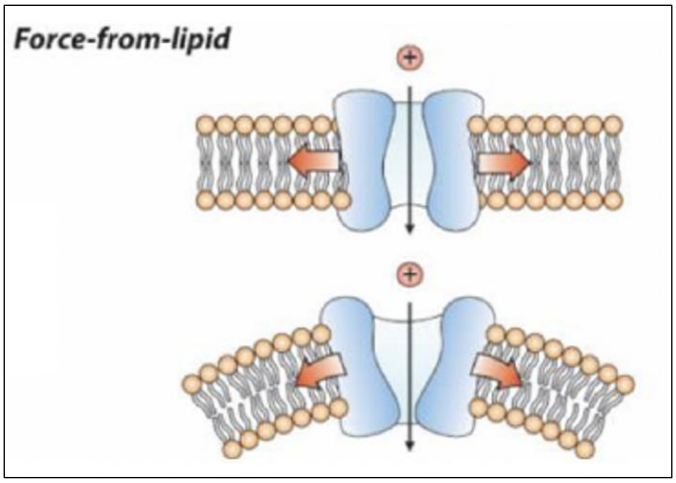

Figure 6.

The force-from-lipid (FFL) ion channel opening model works through phospholipid head and acyl tail interactions creating forces within the phospholipid bilayer to pull the ion channel open to allow ion influx and signal transduction.

(Figure sourced from;[65]).

Piezo1 is a key ion channel in mechanotransduction, it is known to control Klf2 and Notch signalling activity and regulates YAP1 localisation. Piezo1 channel opening allows an influx of Ca^{2+} ion concentrations in VSMC cytoplasm's which stimulates transglutaminase II (TG2) activity [66]. TG2 is involved in ECM and cytoskeletal remodelling through protein crosslinking facilitated by lysine-glutamine isopeptide bonds [48].

Angiotensin II plays a key role in transduction pathways in VSMCs, it is a vasoconstrictor due to its ability to regulate the renin-angiotensin system which is responsible for regulating blood pressure, vascular tone and salt, ion and water balance [67]. Angiotensin II binds to AT1 and AT2 receptors, binding to these receptors stimulates G-protein activity and activates downstream signalling pathways which are known to stimulate tyrosine kinases including Janus kinases (JAK) and focal adhesion kinases (FAK) via activation of receptor tyrosine kinases [68].

1.6 Protein synthesis and post translational modifications

Proteins are made from DNA that is transcribed into messenger RNA (mRNA) that is translocated to the ribosome where the nucleotide sequence is translated and peptide bonds form creating a polypeptide chain [69]. Transfer RNAs (tRNA) are adaptor molecules that bind to the surface of amino acids and codons to facilitate mRNA translation, tRNAs line up amino acids in the correct order and peptide bonds form between amino acids forming a polypeptide chain. The ribosome is made of a small and large subunit, the small subunit is responsible for translation and tRNA binding codons in the correct order. The large subunit facilitates peptide bond formation between amino acids forming the polypeptide chains [70]. The polypeptide chain is transported from the ribosome to the endoplasmic reticulum (ER) where it is folded into a protein. Polypeptide chains have a signal recognition particle which is recognised and binds to a receptor protein on the ER surface [71]. Binding induces translocated on the polypeptide chain into the lumen of the ER through hydrophilic transmembrane protein translocators in the ER [72]. In the ER lumen, the proteins are folded, and N-linked oligosaccharides are added. These oligosaccharides are added to serve as a marker for protein folding completion, ER chaperones bind to the N-linked oligosaccharides on incomplete folded proteins and prevent them from leaving the ER [73]. ER glucosidases act as checkpoints in the ER and remove glucose units bound to the protein, if folded correctly, all three glucose units on the protein will dissociate and the chaperones detach from the protein allowing it to translocate out of the nucleus. Misfolded proteins trigger the unfolded protein response (UPR) where the proteins are degraded by proteasomes in the cytosol of the ER and destroyed [74]. Once folded proteins are then modified, packaged and secreted by the Golgi apparatus. The Golgi is comprised of 3 sections; the cis-Golgi network is responsible for receiving proteins from the ER and the cis-medial-trans-Golgi cisternae contains glycosylation enzymes that PTMs proteins by adding sugars to the amino acids of the protein [75]. The trans-Golgi network (TGN) is responsible for sorting, packaging and excreting proteins to their correct destination in the cell (**Figure 8**).
The glycosylation of proteins is a key PTM in protein synthesis as it improves protein stability and can regulate protein solubility depending on the protein role and function, it also serves

as a checkpoint to ensure protein folding and aids in protein transport through the Golgi [76]. Acetylation in the Golgi occurs through the addition of an acetyl group from acetyl coenzyme A which is produced in the cytosol. The acetyl group modifies the protein at the N-terminal by histone acetyltransferase type B protein 4 (HAT4), acetyl groups are also removed by histone deacetylases (HDACs) [77]. Acetylation of proteins can alter the properties of proteins including structure through conformational changes, protein stability and localisation [78]. Methylation occurs on the N-terminal of arginine and lysine in the proteins and is carried out by DNA methyltransferases (DNMT) such as S-adenosylmethionine (SAM) [79]. Methylation is involved in regulating gene expression, gene silencing, transcription, protein translocation and protein function. Methylation is strongly linked to VSMC remodelling and atherosclerosis through DNMT-mediated VSMC phenotypic switching to dedifferentiated synthetic phenotypes [80]. UBE3A encodes E3 ubiquitin ligase Ube3a which binds ubiquitin to proteins to modify the function of the protein or ubiquitinate the protein to degrade the protein [81]. Ubiquitination is often involved in the DNA damage response pathway as it activates NF-kB signalling which results in the activation of inflammation-specific response genes in VSMCs which respond to MMPs [82].

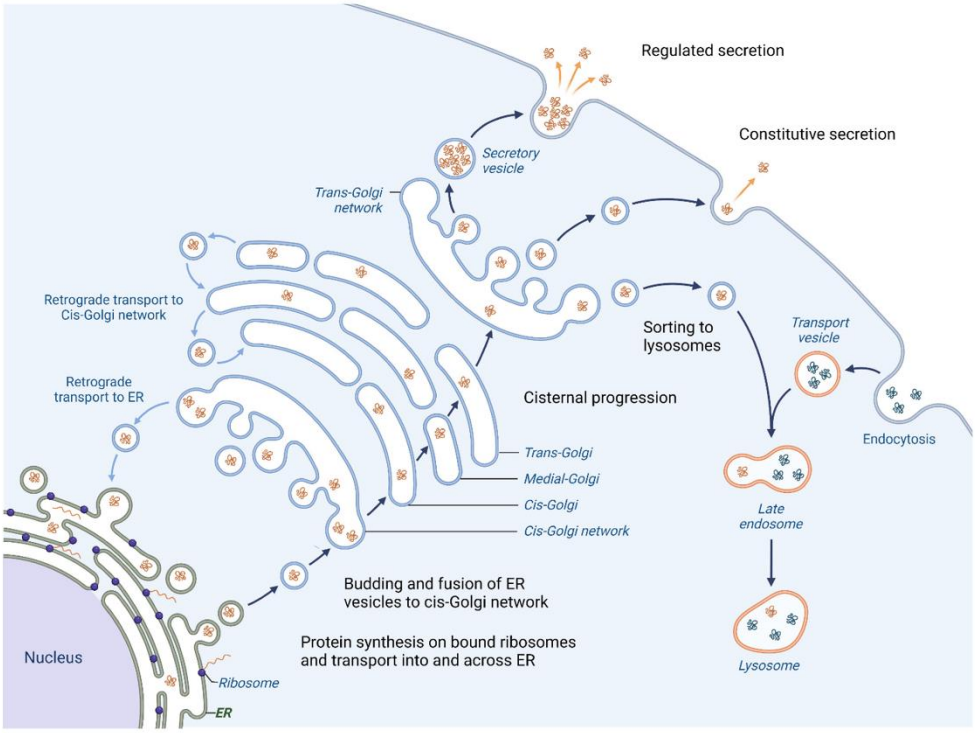

Figure 8.
Protein synthesis starts from mRNA transcription in the nucleus, the mRNA moves to the ribosome where the mRNA is translated into a polypeptide chain. The polypeptide chain translocates to the endoplasmic reticulum (ER) where the chain is folded into a protein. Finally, the protein moves to the Golgi apparatus where it is post-translationally modified and packed into a vesicle and is transported.
(Figure sourced from;[83]).

Histones are key regulators in gene expression, they are modified in order to regulate whether a gene is activated or repressed. This is achieved through either acetylation or methylation; acetylation exposes transcription factor binding sites allowing genes to be activated and methylation represses genes. Histone acetylation is induced through histone acetyltransferases (HATs), these HATs catalyse the addition of an acetyl group to a conserved lysine residue. This acetylation causes histone affinity for DNA to reduce resulting in the histone unwinding which exposes the chromatin structure of the DNA allowing transcription factors to bind [84]. H3K9 is acetylated by p300 and deacetylated by HDAC3 and SIRT1 [85]. The acetylation of H3K9 is important in the regulation of phenotypic switching in VSMCs. Histone methylation involves the addition of a methyl group, this usually occurs at the gene promoter region and results in the inhibition of gene transcription [86]. Studies into H3K9 methylation discovered that reduced methylation promoted the binding of activation protein 1 (AP-1) and nuclear factor kappa-light-chain-enhancer of activated B cells (NFκB) transcription factors which activate inflammation-specific response genes in VSMCs which respond to MMPs or IL6 that are released in VD and when VSMCs undergo cell damage. Suggesting reduced methylation and increased acetylation could be key to reducing MMP/IL6 expression in aged and diseased cells [87].

1.7 VSMC microtubule structure and function

Microtubules play a key role in VSMC signalling and the cytoskeleton and are a crucial component of the aorta. They consist of α and β heterodimers which polymerise together to form a protofilament [88]. A microtubule consists of 13 protofilaments which form a lattice of tubulin filaments (**Figure 7**). Microtubules are in a state of dynamic instability due to the fact they must expand and contract in order to change size [89]. In addition to this, to withstand the high mechanical pressure of the aorta microtubules are acetylated to reinforce themselves and stabilise in response [90]. Stability is regulated through post-translational modifications (PTM) of the α and β subunits and microtubule-associated proteins (MAPS) which work to regulate many processes including stability, dynamics, binding affinity and more [91]. PTM can directly modify the functionality of microtubules and these PTMs include acetylation, phosphorylation, ubiquitylation, methylation, polyamination and palmitoylation. Tubulin acetylation is thought to induce associations between tubulin monomers and results in increased microtubule stability [92]. Previous studies have shown mixed results relating to the impacts of α-tubulin acetylation. However, the most commonly seen response to the acetylation of α-tubulin results in increased microtubule stability [93]. This is achieved through acetylating K40 in polymerized tubulin monomers and causing a conformational change in the Lysine 40 binding site, this promotes lateral associations between tubulin monomers to

increase the stability of the microtubule [94 95]. This increased stability allows the microtubules to be more resistant to mechanical damage and to function more effectively against increased stress and mechanical load in the aorta.

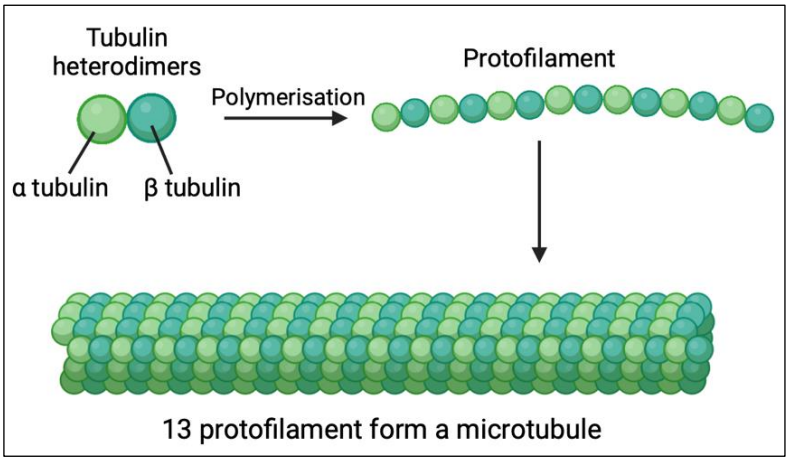

Figure 7.

Structure of a microtubule, alpha and beta tubulin heterodimers polymerase to form into a protofilament. Thirteen protofilaments bind together to form a single microtubule.
(Figure generated in Biorender.com)

Acetylation in microtubules occurs when there is an addition of an acetyl functional group into the lysine residues of α-tubulin and both histone and non-histone proteins. However, this can be inhibited using Histone deacetylases (HDACs). HDACS are enzymes that remove acetyl groups from lysine residues to deacetylate them [96]. There are also HDAC inhibitors which prevent de-acetylation, which is important in regulating other PTMs. Acetylation prevents ubiquitination-dependent proteasome-mediated protein degradation from occurring and as a result, can improve protein stability in many proteins. HDACs can remove the acetyl group exposing the lysine to ubiquitin and induce protein degradation [97]. In α tubulin, the most common acetylation is in a region known as K40, which is located between the p37 and D47 residues of the protein [98]. The acetylation of α tubulin is caused by α-tubulin acetyltransferase 1 (αTAT1) and is deacetylated by HDAC6 [99].

1.8 Tau

Tau is a protein that binds to and stabilises microtubules, during aging Tau is known to aggregate and can no longer bind to microtubules resulting in destabilisation. Tau has been linked between CVD and neuropathies, vascular dementia leads to reduced blood flow in the vasculature [100]. It results in high blood pressure and reduced oxygen levels in the brain and can dramatically reduce life expectancy. Studies into vascular dementia (VD) have linked Tau

activity to increased risk of VD through Tau hyperphosphorylation [101]. In aged VSMCs Tau accumulation and phosphorylation occur, this can be used as a marker for ageing in cells.
When Tau undergoes phosphorylation, there is a proline to leucine substitution that occurs in several residues which induces a conformational change in the protein [102]. The misfolding of Tau proteins has been strongly linked to its hyperphosphorylation which can induce further conformational changes. Phosphorylation of Tau at Thr231 induces conformational changes that cause misfolding to occur and result in additional conformational changes at subsequent sites [103]. Additionally, due to the conformational changes to Tau, its binding affinity and ability to promote microtubule assembly are significantly reduced [104]. Tau is phosphorylated by several kinases including GSK3β, c-Jun N-terminal kinase (JNK) and Cyclin-dependent kinase 5 (Cdk5), with GSK3β being a key mediator of TAU phosphorylation [105]. Once phosphorylated Tau detaches from microtubules previously bound to and can no longer bind to microtubules, this destabilises both the microtubule and microtubule cytoskeleton. It has also been found Tau aggregates reduce levels of acetylated α-tubulin, which is known to increase microtubule stability [106].

1.9 Senescence and cell death

Cell senescence and apoptosis are primarily caused by DNA damage, this is often induced during the cell cycle at checkpoint 2 by checkpoint kinase 2 (Chk2) [107]. Chk2 is an enzyme encoded by the *CHEK2* gene which is crucial in the cell cycle as it is responsible for inducing cell cycle arrest and induces apoptosis in cells via DNA damage [108]. DNA damage is the main process of cellular ageing and senescence and has been linked to the development of many cardiovascular diseases such as atherosclerosis [109]. It involves the deletion of DNA sections, extrusion of micronuclei, Single and double-stranded breaks and nucleotide modifications which all result in cell death [107]. Senescence is the process of cells becoming no longer proliferatively active. This means that they no longer proliferate to form new cells or replace damaged or dead cells. Additionally, senescent cells remain metabolically active and can promote inflammation through senescence-associated secretory phenotype (SASP), these give rise to the production of MMPs and IL6 which contribute towards cell death via apoptosis [110]. VSMC senescence can be induced by a number of factors including DNA damage, inflammation, oxidative stress and angiotensin II [110]. DNA damage involves single and double-stranded breaks (DSB), deletion of DNA sections and extrusion of micronuclei.
NAT10 is heavily linked with contributing to cell senescence through micronuclei activating the senescence-associated secretory phenotype (SASP) in VSMCs [111]. NAT10 is known to increase micronuclei formation in cells through DNA replication, micronuclei activate the cGAS-cGAMP-STING pathway. This pathway works by micronuclei or cytosolic DNA

combining by cGAS, catalyzing GTP and ATP to form cGAMP, which activates STING, enabling NFκB activity, inducing the stimulation and release of SASP's including proinflammatory factors such as cytokines, proteases and chemokines [112]. The proinflammatory factors released include MMPs and IL6 which contribute to cell senescence and eventually cell death.

When DNA damage is induced, it activates the DNA damage response pathway (DDR), this pathway activates a cascade of proteins that act as sensors and effectors to induce a repair or death pathway. DDR sensors can dictate if the cell cycle should be stopped to allow for DNA repair and directly induce repair, or it can induce senescence or apoptosis if the damage detected is unrepairable [113]. Ataxia telangiectasia–mutated protein (ATM) pathway and similar kinases are recruited by sensor complexes, which induce the DDR through activation of multiple downstream effectors. ATM pathway continuously works in the cell cycle, when DNA damage is detected in a break site it is recognised by the MRN sensor complex which activates ATM [114]. ATM phosphorylates H2AX and induces downstream activation of downstream effectors such as P53-binding protein 1 (53BP1) which promotes checkpoint activation and repair. The tumour suppressor protein p53 is a key sensor of DNA damage and can induce cell cycle arrest or senescence and apoptosis [115]. It is these effectors that determine whether the damage is repairable or not, and in turn they induce cycle arrest and repair or induce senescence and apoptosis.

Annexin A3 (ANXa3) is a protein encoded by the *ANXA3* gene and plays an important role in VSMCs through the regulation of the JNK pathway. Past studies have linked ANXa3 to tumour formation in liver cancer through JNK signalling activation [116]. Additionally, wang *et al*., found that the inhibition of ANXa3 through Si-ANXA3 inhibited the phosphorylation and activation of the JNK signalling pathway and resulted in the promotion of VSMC cell proliferation and a reduction in VSMC apoptosis [117]. JNK signalling is known to induce apoptosis in cells through multiple mechanisms; JNK phosphorylates BCL2 to inhibit its anti-apoptotic function. Additionally, JNK can stimulate the activation of c-JUN and other transcription factors which induce apoptosis [118].

1.10 Experimental design

My study utilised the use of polyacrylamide hydrogels to more accurately model the ECM environment of the aorta. By manipulating the ratio of acrylamide to bis-acrylamide the stiffness of the gels can be controlled. 2kPa represents a very soft aorta and is the stiffness cells experience during migration in atherosclerosis which results in the formation of atherosclerotic plaques. 12kPa represents a healthy aorta, healthy arteries are between 10-

20kPa in stiffness, therefore 12kPa was chosen as these gels can be produced consistently at this stiffness and 12kPa is more representative of a younger and healthier stiffness than 20kPa. 72kPa represents an aged or diseased aorta, between 60-200kPa is the stiffness of an aged or diseased aorta, 72kPa was chosen as it is closer to stiffness seen in aged aortas, 200kPa Is more representative of severely diseased aorta rather than aged. The stiffness of the hydrogels was tested and confirmed using atomic force microscopy (AFM).

Due to the fact, VSMCs are highly mechanosensitive and respond to changes in ECM stiffness, they need to be grown on a substrate of similar stiffness to what they experience in the aorta. Glass coverslips and plastic 6 well plates have a stiffness 10000x stiffer than a healthy aorta **(Figure 9)**. Therefore, by controlling the stiffness of the gels, cells can be grown in conditions representative of young healthy aged aortas (12kPa) or aged and diseased aortas (72kPa). After the age of 50 in humans the aorta is known to stiffen and become aged. Additionally, the use of collagen type 1 as the ECM component in the hydrogels is an advantage as it is the most abundant protein in the ECM of VSMCs [119]. Being able to use collagen 1 as the ECM component in hydrogels allows us to more accurately model the ECM environment in vitro.

There are limitations to my study, one limitation is the use of Sulfo-SANPAH to crosslink proteins onto the hydrogels, it is known to have limited solubility which results in variable effectiveness of the crosslinking step of hydrogel fabrication and can impact how the gels work [120]. Additionally, the hydrogel model is only 2 dimensional as the cells only have lateral interactions, whereas within the aorta VSMCs are within a 3-dimensional environment. Furthermore, hydrogels only have 1 type of ECM component which is collagen 1 and whilst it's the most abundant component, it is not the only one present in the ECM. Therefore, the hydrogel model is unable to model the full composition of the ECM and could lack interactions between VSMCs and ECM proteins.

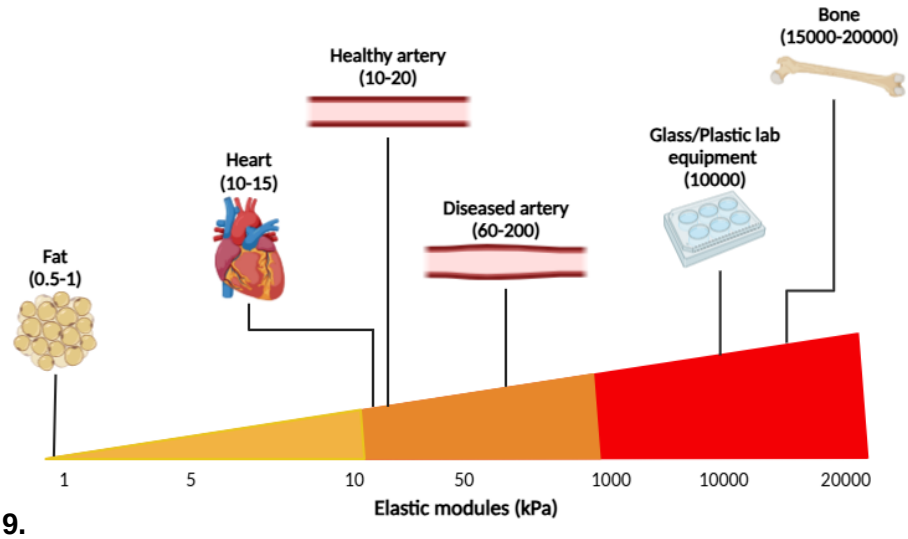

Figure 9.

Stiffness comparison measured in kilopascals (kPa). Stiffness was measured using atomic force microscopy.

(Figure generated in Biorender.com)

1.11 Hypothesis and aims

Hypothesis:

Gene expression and protein modification are known to change in response to a variety of extracellular and intracellular signals. Therefore, the overall hypothesis of this thesis is that; protein levels and protein modification levels will increase in response to matrix stiffness and ageing.

Aims:

To determine whether:

1. Tubulin acetylation increases in response to matrix stiffness
2. Tau and GSK3β phosphorylation increases in response to VSMC ageing
3. Histone acetylation and methylation increases in response to matrix stiffness and ageing
4. Protein levels of NAT10, Chk2, PDLIM1 and ANXa3 increase in response to matrix stiffness and ageing.

VSMCs of different passage numbers were grown on hydrogels of different stiffnesses. Specifically, 2kPa hydrogels modelled a soft environment, 12kPa hydrogels modelled healthy stiffness and 72kPa hydrogels modelled aged stiffness. For ageing studies, low passage (P8) were compared to high passage (P16) VSMCs. Western blot analysis was formed on whole cell lysates. Proteins and modified forms of the proteins were detected using commercially available total and modification specific antibodies.

2. Methods

2.1 Vascular Smooth Muscle Cell Culture and SiRNA Knockdowns

Human aortic VSMCs were purchased from cell applications Inc., the cells used were pooled from 3 different patients aged 25-60 who all had no underlying cardiovascular health conditions. Cells were grown in smooth muscle cell growth media (Cell Applications Inc.) with growth supplement (Cell Applications Inc.) at 37°C and 5% CO_2 in an incubator. Cells are incubated for 3-5 days to reach confluence, once confluent (>80%), cells can be split. Confluent cells can be split by first washing using Earls Balanced Salt wash (Thermo) and trypsinised (Thermo) to detach cells from the flask and incubated for 3 minutes at 37°C and 5% CO_2. Once trypsinised, growth media with supplement is added to neutralise the trypsin and bring the volume of the flask to the correct amount for splitting, half the volume is pipetted

into a new flask. Once split cells are then returned to the incubator to grow. SiRNA treatments required cells to be seeded onto plastic T-25 flasks 24 hours prior to SiRNA knockdown. VSMCs were treated using various SiFACE1 treatments (QIAGEN), a control, OLIG2 and OLIG4 treatments were used to knockdown FACE1. Each treatment consisted of 28µl of HiPerFect (QIAGEN), 2µl of either a control mix or an Oligo 2/4 primer and 430µl of basal media (Cell Applications Inc.). Once the treatment was mixed, it was left to incubate for 15 minutes at room temperature before being pipetted onto each flask of cells. The treated cells were then incubated for 72 hours at 37°C and 5% CO_2 before cell lysates were produced by adding 2x Laemmli loading buffer, and the cells scraped off using a cell scraper. Lysates were then extracted and stored at -20°C. Cells used for hydrogels and SiRNA FACE1 knockdown were from passages 7-12.

2.2 Polyacrylamide hydrogel fabrication

Standard 30mm coverslips were first activated by treating with (3-aminopropyl)triethoxysilane for 2 minutes and then washed 3 times with dH2O. Next, the coverslips were fixed in 0.5% glutaraldehyde for 40 minutes before another 3 washes with dH2O, once washed the coverslips were then left to air dry for a minimum of 30 minutes. Once activated the coverslips are then ready to have hydrogels made onto them, a hydrogel buffer mix is used to determine the stiffness of the gels, 2 kPa (5% acrylamide with 0.1% bis-acrylamide in water), 12 kPa (7.5% acrylamide with 0.15% bis-acrylamide in water) and 72 kPa (10% acrylamide with 0.5% bis-acrylamide in water) is mixed with 10% APS (1:100) and TEMED (1:1000) and 50µl was pipetted onto a clean microscopy slide and covered by an activated coverslip. The stiffness of the hydrogels was tested and confirmed by Minaisah et al [121]. After 90 seconds the hydrogels were checked to see if the gel had set, if set the gels were removed from the slide and placed into a 6-well plate and washed 3 times with dH2O. The hydrogels were then crosslinked using sulfo-SANPAH (1:3000) in PBS for 5 minutes and then sterilised in a UV steriliser for 30 minutes. Next, the gels were washed with PBS and functionalised using collagen type 1 (1:30) for 10 minutes. Finally, cells are seeded onto the hydrogels using standard techniques.

2.3 Cell lysate preparation

Cell lysate samples were obtained using a diluted 4x Laemmli's buffer and 1x PBS made in a 1:1 ratio. Laemmli's buffer (4x) was comprised of SDS (8%), 2-mercaptoethanol (20%), glycerol (40%), Tris base (3.04%) and bromophenol blue (0.008%). Tris base was prepared by mixing Tris with d.H2O (20%) and pH balanced to 6.8 using hydrochloric acid (HCl). The diluted laemmli's buffer was added onto the cells either in a 6 well plate (150µl of laemmli's

buffer per well), a T-25 flask (300µl of laemmli's buffer) or a T-75 flask (600µl laemmli's buffer). The buffer was left for 60 seconds at room temperature, then the cells were scraped using a cell scraper (thermo) and pipetted into a labelled Eppendorf. When lysing from hydrogels, samples were sonicated for 15 seconds to break down any remaining gels in the sample.
Before use in western blots, lysates were boiled at 90ºC for 5 minutes before being spun down in a centrifuge at 12,000 rpm for 45-60 seconds.

2.4 Western blotting

Lysates from aortic tissue samples were subjected to Western blotting analysis. An equal amount of protein for each sample was loaded into a 10% precast sodium dodecyl sulfate-polyacrylamide denatured gels, the tank was then filled with 800ml 1x TruPAGE Tris-MOPS SDS Running buffer with dH2O and ran at 120v and 400mA for 70 minutes. Once the gels had run for the desired period, the gels were placed into a transfer pack and filled with 800ml Tru-PAGE transfer buffer and transferred onto a nitrocellulose polyvinylidene difluoride (PVDF) membrane for 2hrs at 30v and 400mA. Once transferred the nitrocellulose membrane was blocked with 5% Milk with Tris-Buffered Saline with 0.1% tween (TBST) (Merck) for 60 minutes. The membranes were incubated overnight at 4°C in 5% milk with TBST and a primary antibody. The membranes were then washed with TBST for 30 minutes, changing the TBST every 3 minutes, and then incubated with 5% milk in TBST and a Horseradish peroxide (HRP) labelled monoclonal secondary antibody for 120 minutes at room temperature in the dark. The membranes were then washed 10 times for 3 minutes per wash. An ECL detection reagent was prepared and 500-1000µl was pipetted onto each membrane. Membranes were imaged using an automated imaging system (Bio-Rad) and analysed using Fiji software.

2.5 Statistical analysis

All statistical analysis was carried out using GraphPad Prism version 10.4.1 and confirmed using SPSS software. Graphs show combined data from multiple repeats, error bars show standard error of means. Data sets comparing 1 variable were analysed using a paired t-test as the data analysed is two-tailed, paired and parametric as data sets are collected in 3 repeats. Data sets containing multiple variables were analysed using a One-way ANOVA with a Tukey's post-hoc test, as the data used has 3 repeats per variable.

3. Results

3.1 polyacrylamide hydrogel validation

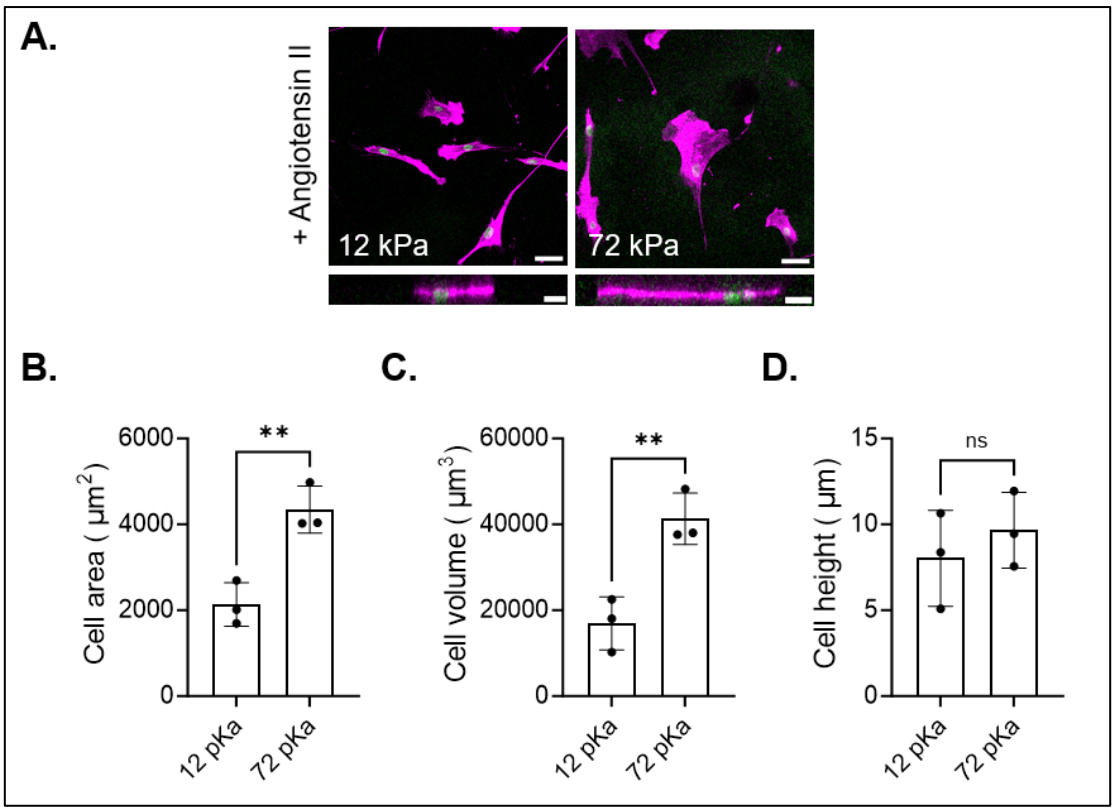

Figure 10. Representative images of isolated angiotensin II stimulated VSMCs cultured on 12 and 72 kPa polyacrylamide hydrogels. The actin cytoskeleton (purple) and DAPI-labelled nuclei (green) are shown. Top panels show representative *xy* images of VSMC area, and bottom panels show representative *xz* images of VSMC height. Scale bars: 50 µm (top); 20 µm (bottom). **(A)**. Analysis was carried out to determine cell area **(B)**, cell volume **(C)** and cell height **(D)**. statistical analysis was carried out using an unpaired t-test.
Figure adapted from; [122]

Cell imaging shows a visual increase in cell size in 72kPa compared to 12kPa **(Figure 10A)** In response to increased matrix stiffness, cell area, volume and height all increased between 12kPa and 72kPa with the increase in cell volume significantly increasing between 12kPa and 72kPa **(Figure 10C)**.

3.2 SiRNA knockdown confirmation

The SiRNA knockdown of FACE1 which is responsible for the conversion of pre-lamin A into mature lamin A was tested to confirm whether the knockdown had been successful. Upon

probing a western blot for pre-lamin A **(Figure 11),** there were bands present in the control sample and in both the OLIG2 and OLIG4 knockdowns. Indicating the knockdown had been unsuccessful as the control should have lower levels of pre-lamin A.

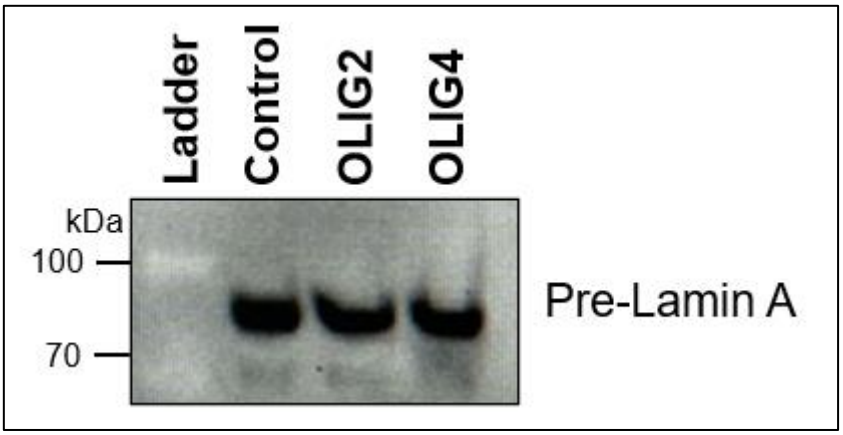

Figure 11. A preliminary western blot image of cells treated with SiRNA FACE1 knockdown and probed with pre-lamin A to confirm if FACE1 knockdown was successful. Pre-lamin A has a molecular weight of 72kDa. This experiment was carried out a single time (N=1).

3.3 Microtubule stability

In this study, polyacrylamide hydrogels were used as they allow the ability to control the stiffness of the gels to accurately model the stiffness of the extracellular matrix of the aorta. Cells were grown on both healthy pliable (12 kPa) and aged rigid (72 kPa) hydrogels and probed with acetylated α-tubulin and total α-tubulin to observe changes (**Figure 12A**). When investigating acetylated α-tubulin (**Figure 12B**) there was no significant change in levels of acetylated α-tubulin in the 72 kPa compared to the 12 kPa. When observing levels of total α-tubulin (**Figure 12C**) there was no significant change in the levels of total α-tubulin in the 72 kPa gels compared to the 12 kPa. Additionally, when looking at the difference between acetylated and total α-tubulin (**Figure 12D**), there appeared to be an increase in the 72 kPa compared to the 12 kPa hydrogels.

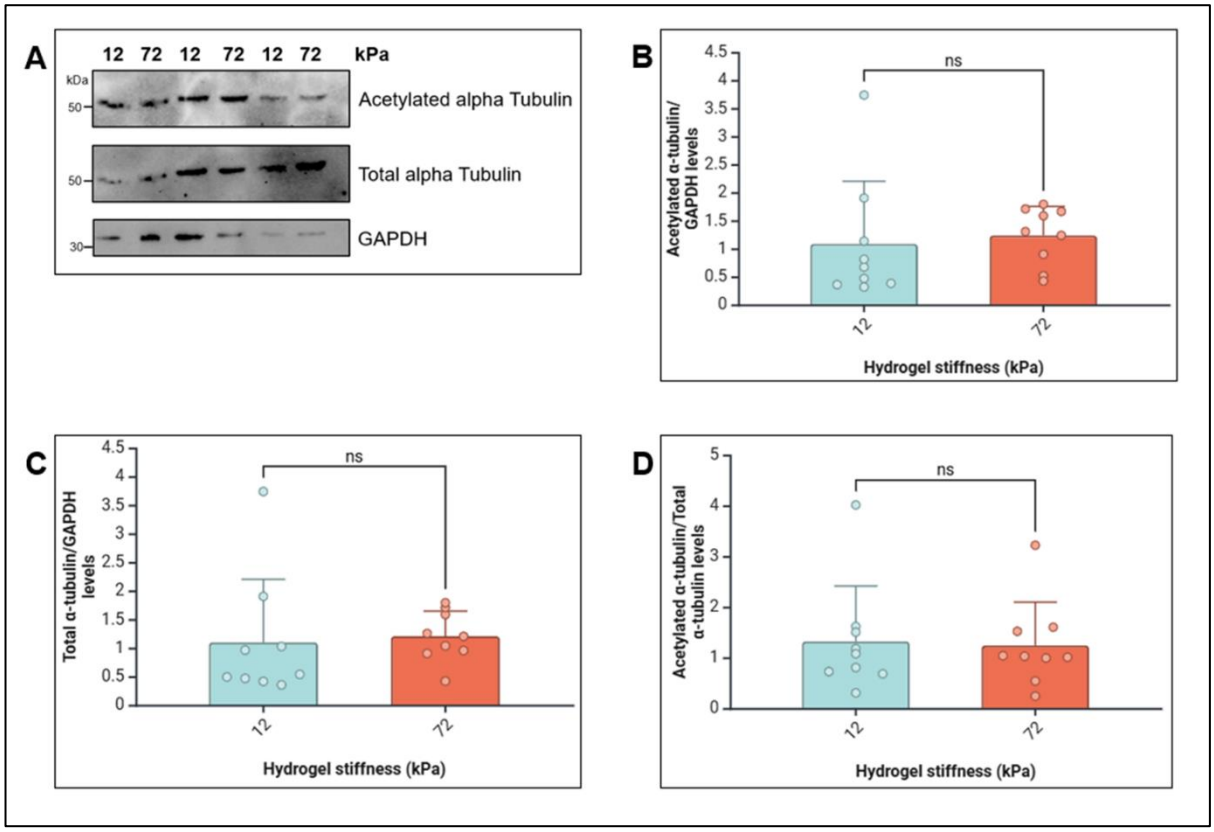

Figure 12. Alpha-tubulin is a heterodimer that forms microtubules with beta-tubulin. **A)** representative western blot images of cells cultured on 12 kPa and 72 kPa hydrogels and probed with acetylated and total alpha-tubulin antibodies. **B)** Representative chart showing an average of the level of acetylated α-tubulin in VSMCs grown on their respective hydrogels. The dots on the graph represent data points for each repeat of the experiment. Acetylated α-tubulin has a molecular weight of 52kDa. **C)** Representative chart showing an average of the level of total α-tubulin in VSMCs. Total α-tubulin has a molecular weight of 50kDa **D)** Representative chart showing an average of the level of acetylated α-tubulin divided α-tubulin by the total α-tubulin in VSMCs. This experiment was repeated 3 times (N=3) and the results were averaged. All statistical analysis was carried out using an unpaired two-tailed t-test.
(All graphs were produced in Biorender.com)

It was investigated if there would be a change in α-tubulin levels in young and aged cells, this was achieved by producing cell lysates from VSMCs at different cell passages. Cells were lysed and collected at passage 8 (P8) and passage 16 (P16) (**Figure 13A**). The older P16 cells (**Figure 13B**) showed slightly higher levels of acetylated α-tubulin in the younger P8 cells compared to the older P16, upon statistical analysis, the increase in level was found to be insignificant. Upon investigation of total α-tubulin levels, there was no significant change in levels of total α-tubulin between the P8 and P16 cells (**Figure 13C**). Finally, when looking at the difference between acetylated and total α-tubulin (**Figure 13D**), there appeared to be an

increase in the P16 compared to the P8, however, this difference was not found to be statistically significant. The data collected in Figures 4 and 5 was carried out in triplicate and averaged out, it contained outliers in the data, however, it could be seen that overall, there were no changes in tubulin acetylation in response to stiffness changes or cell age.

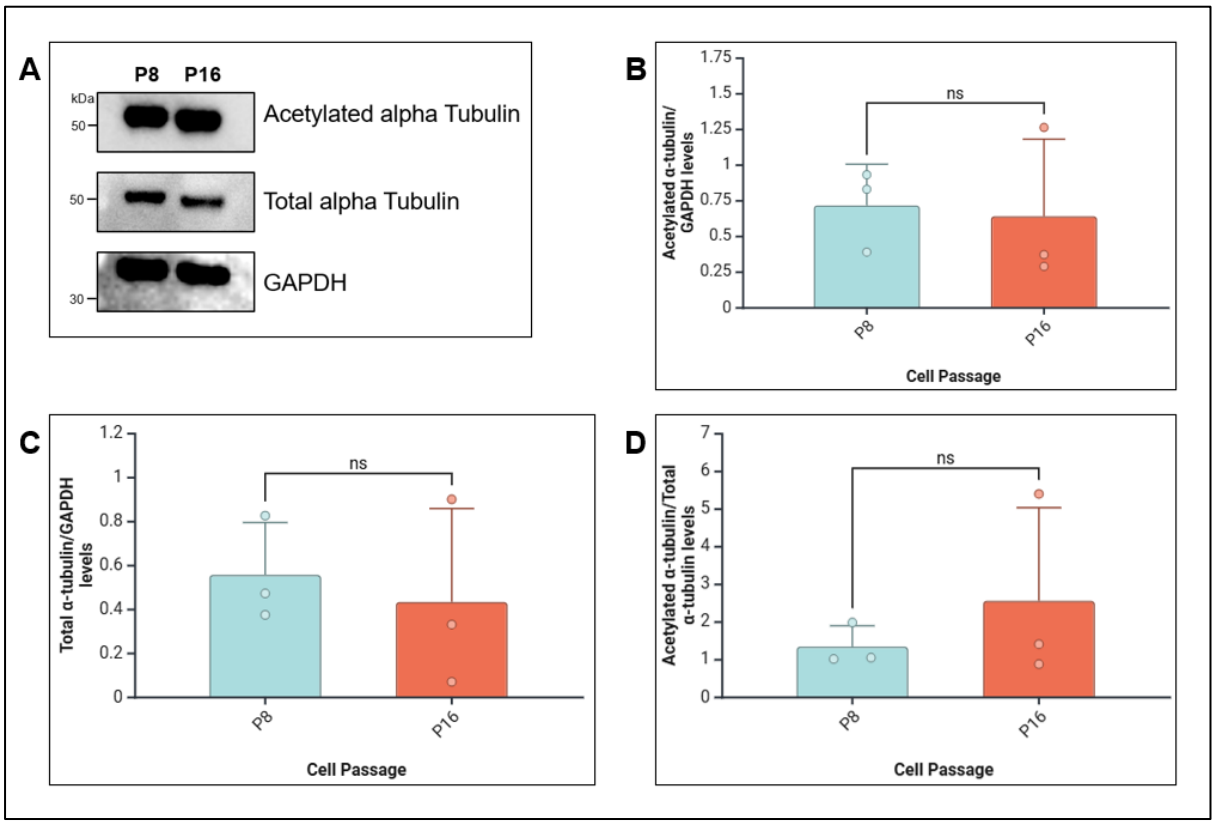

Figure 13. A) representative western blot images of cells from different passage points cultured on plastic. **B)** Representative chart showing an average of the level of acetylated α-tubulin in VSMCs at passage 8 and 16, the dots on the graph represent data points for each repeat of the experiment. Acetylated α-tubulin has a molecular weight of 52kDa. **C)** Representative chart showing an average of the level of total α-tubulin in VSMCs. Total α-tubulin has a molecular weight of 50kDa. **D)** Representative chart showing an average of the level of acetylated α-tubulin divided α-tubulin by the total α-tubulin in VSMCs. This experiment was repeated 3 times (N=3) and the results were averaged. All statistical analysis was carried out on the mean data using an unpaired two-tailed t-test.
(All graphs were produced in Biorender.com)

3.4 Tau phosphorylation

Tau is a protein known to bind to microtubules and increase stability, in ageing Tau is known to both aggregate and phosphorylate. Both of these processes prevent Tau from binding to microtubules and result in reduced stability of microtubules and the cytoskeleton. The first experiment was carried out to investigate the levels of Tau phosphorylation at different sites and see if mimicked ageing had an impact on SiRNA FACE1 knockdown would impact phosphorylation levels. (**Figure 14A**). Upon probing for phospho-Tau 396 (**Figure 14B**) there was no significant change in levels of phospho-Tau 396 in the OLIG2 and OLIG4 cell lysates compared to the control. This was also found to be the same when probing for phospho-Tau 202 (**Figure 14C**). Phospho-GSK3β (**Figure 14D**) also had no change in levels in OLIG2 or OLIG4.

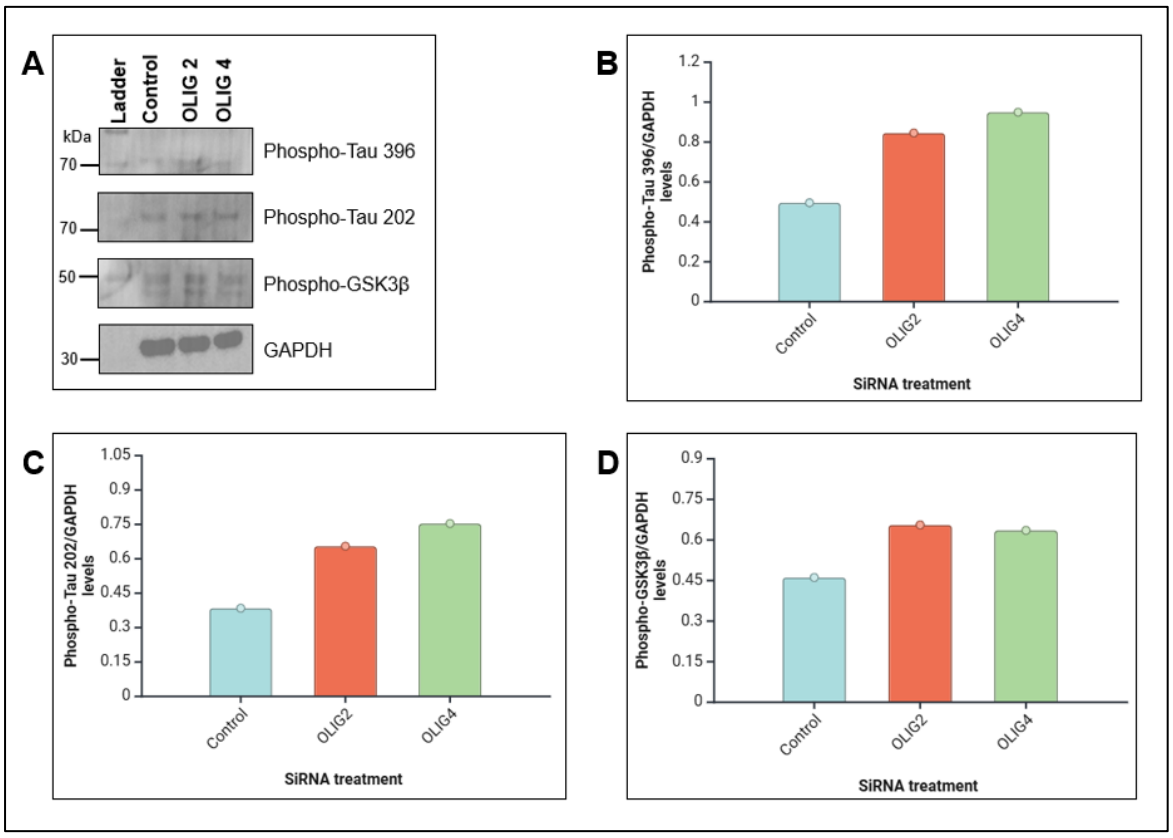

Figure 14. **A)** Western blots of VSMCs treated with an SiFACE1 knockdown and probed with phospho-Tau 396, 202 and phospho-GSK3β. **B)** Chart showing levels of phospho-Tau 396 in VSMCs. Phospho-Tau 396 has a molecular weight of 78kDa. **C)** Chart showing levels of phospho-Tau 202 in VSMCs. Phospho-Tau 202 has a molecular weight of 79kDa. **D)** Chart showing levels of phospho-GSK3β in VSMCs. Phospho-GSK3β has a molecular 46kDa. This experiment was preliminary and was not repeated (N=1) and therefore no statistical analysis was carried out.
(All graphs were produced in Biorender.com)

3.5 H3K9 modifications

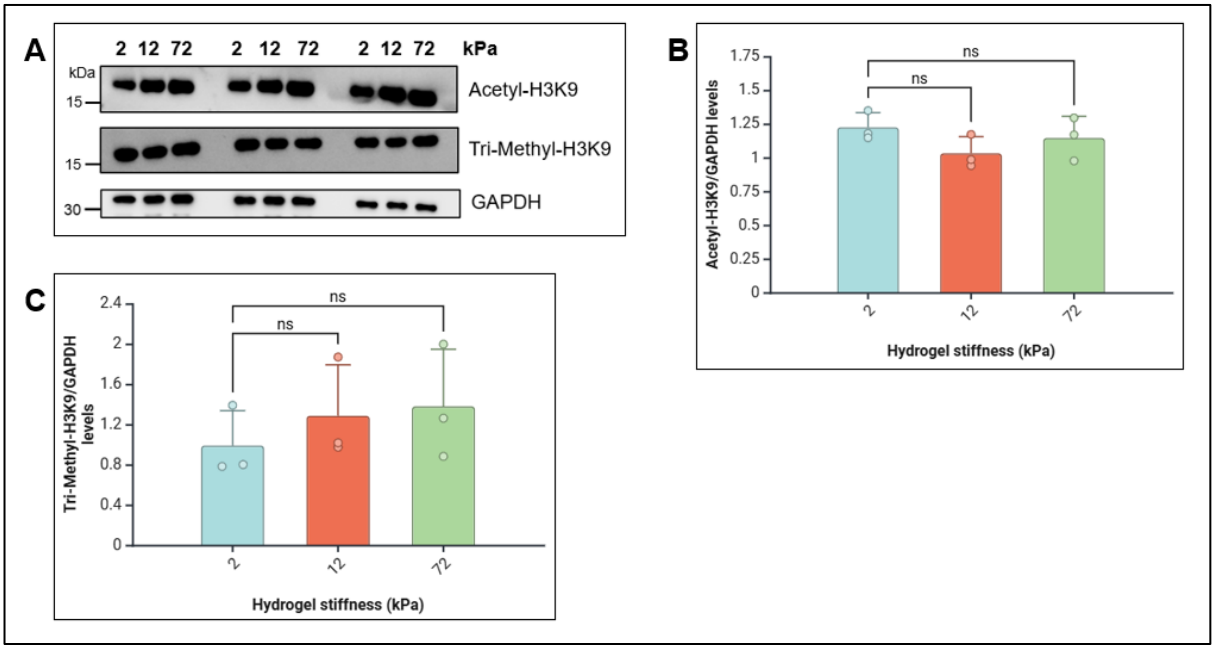

Figure 15. A) representative western blot images of cell lysates collected from VSMCs grown on 2 kPa, 12 kPa and 72 kPa hydrogels and probed with acetyl-H3K9 and tri-methyl-H3K9 antibodies. **B)** A representative graph showing acetyl-H3K9 levels in VSMCs on 2, 12 and 72 kPa hydrogels, the dots on the graph represent data points for each repeat of the experiment. Acetyl-H3K9 has a molecular weight of 17kDa. **C)** A representative graph showing tri-methyl-H3K9 levels in VSMCs on 2, 12 and 72 kPa hydrogels Tri-Methyl-H3K9 has a molecular weight of 17kDa. This experiment was repeated 3 times (N=3) and the results were averaged and normalised to the control GAPDH. All statistical analysis was carried out on the mean data using a one-way ANOVA test.
All graphs were produced in Biorender.com)

It was investigated if histone modifications are impacted by matrix stiffness in VSMCs, cell lysates from VSMCs grown on 2, 12 and 72 kPa hydrogels were run on a western blot and probed with an acetylated-H3K9 and a tri-methylated-H3K9 antibody (**Figure 15A**). It was found that there was an observed change in acetylation levels between 2 and 72 kPa, however, this was not statistically significant (**Figure 15B**). However, there was a significant increase in tri-methyl-H3K9 levels in response to stiffness increase between 2 kPa and 12 kPa and a further non-significant increase of 12 kPa to 72 kPa (**Figure 15C**).

Additionally, it was investigated if the age of VSMCs impacted histone modifications, cell lysates were collected from cells grown at passage 8 and passage 16 and then run on a western blot and probed with acetylated-H3K9 and a tri-methylated-H3K9 antibody (**Figure 16A**). It was found that there was an increase in the levels of acetyl-H3K9 in the older passage

16 cells compared to the younger passage 8 cells (**Figure 16B**). There was also an increase in the levels of tri-methyl-H3K9 in the passage 16 cells compared to the passage 8 cells (**Figure 16C**). However, both increases were not found to be statistically significant.

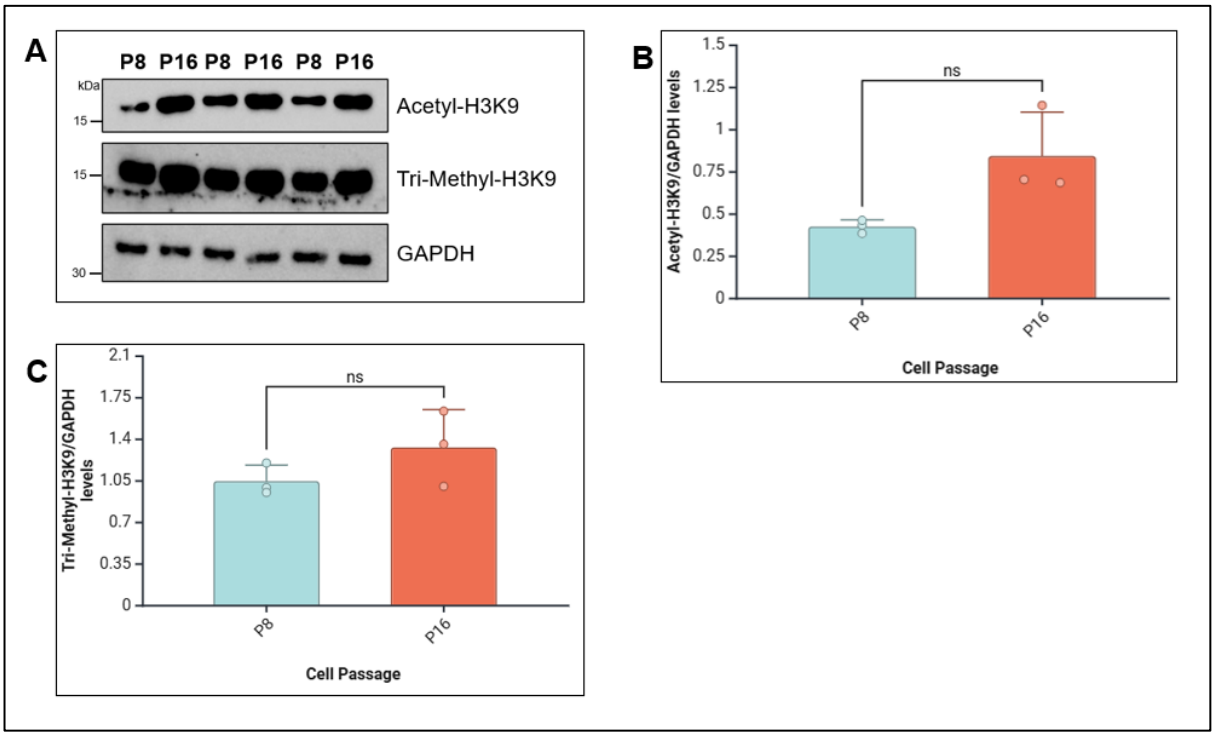

Figure 16. A) Representative western blot images of cell lysates collected from passage 8 and 16, probed with acetyl-H3K9 and tri-methyl-H3K9 antibodies. **B)** A representative graph showing acetyl-H3K9 levels in VSMCs at passage 8 and 16, the dots on the graph represent data points for each repeat of the experiment. Acetyl-H3K9 has a molecular weight of 17kDa. **C)** A representative graph showing tri-methyl-H3K9 levels in VSMCs at passage 8 and 16. Tri-methyl-H3K9 has a molecular weight of 17kDa. This experiment was repeated 3 times (N=3) and the results were averaged and normalised to the control GAPDH. All statistical analysis was carried out on the mean data using an unpaired two-tailed t-test.
(All graphs were produced in Biorender.com)

3.6 Shared post-translational modification in VSMCs in matrix stiffness response and ageing

Bulk mRNA sequencing (mRNAseq) data collected from human aortic smooth muscle cells grown on 2 and 25 kPa hydrogels showed a range of genes that were upregulated in response to increased stiffness in hASMCs, these included *NAT10*, *PDLIM1, ANXA3* and *CHEK2*

(**Figure 17**). To confirm the RNA changes, VSMCs were grown on 2, 12 and 72 kPa hydrogels and run on a western blot and probed with antibodies raised to the corresponding proteins (**Figure 18A**). NAT10 levels were found to increase from 2 to 12 kPa and then a further increase from 12 to 72 kPa, the increase in NAT10 levels between 2kPa and 12kPa and the further increase from 12kPa to 72kPa were both found to be statistically significant. (**Figure 18B**). Additionally, PDLIM1 levels increased between 2 to 12 kPa, however, there was no change between 12 and 72 kPa (**Figure 18C**). When *ANXA3* levels were investigated, there was an increase between 2 and 12 kPa and another increase from 12 to 72 kPa (**Figure 18D**). Finally, Chk2 levels increased between 2 to 12 kPa and then there was no change from 12 to 72 kPa (**Figure 18E**). Although there were observed changes in levels of all proteins investigated, none were found to be statistically significant. To investigate if these protein level changes were shared in both stiffness response and ageing, cell lysates collected from passages 8 and 16 were used to represent young and old cells (**Figure 19A**). It was found that there was no statistically significant change in NAT10 levels, however, upon visual western blot analysis, there is higher levels of NAT10 in the older P16 cells compared to the younger P8 cells (**Figure 19B**). Moreover, when probing for Chk2 there was an increase in Chk2 levels in the aged P16 compared to the P8 (**Figure 19C**). Both of the antibodies investigated matched the results identified in the matrix stiffness response.

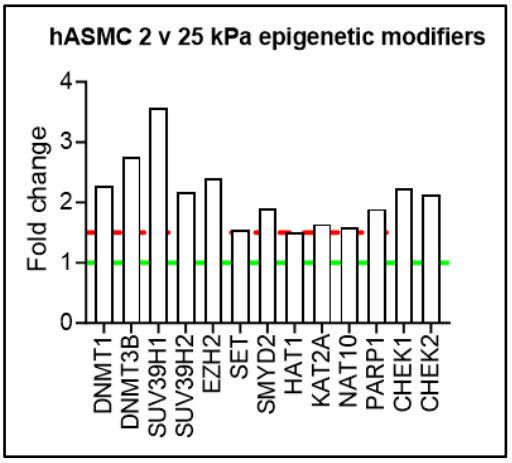

Figure 17. Bulk RNA sequencing (RNAseq) data collected from human aortic smooth muscle cells (hASMC) grown on 2 kPa and 25 kPa hydrogels. Showing a range of genes that were significantly upregulated in response to increased matrix stiffness.
(Figure sourced from;[123])

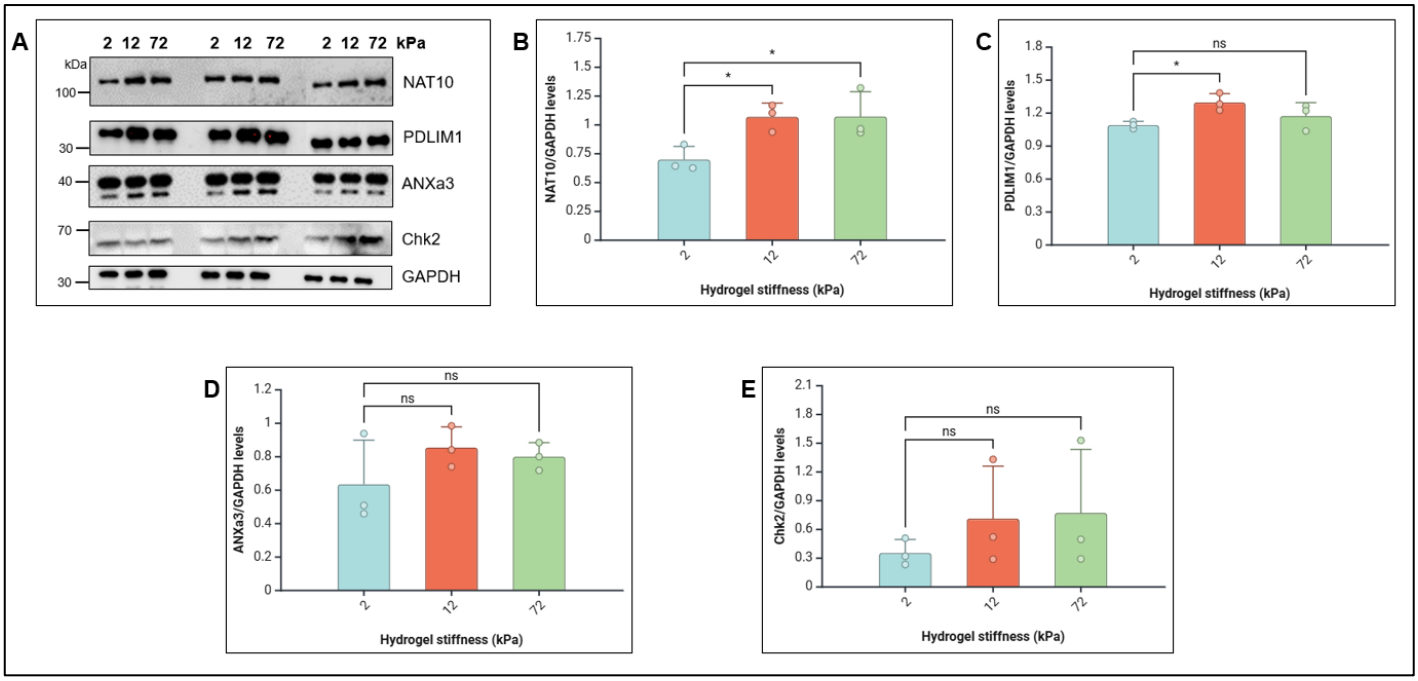

Figure 18. A) Representative western blot of VSMCs grown on 2 kPa, 12 kPa and 72 kPa hydrogels and probed with various antibodies selected from a list of upregulated genes identified in the mRNAseq data set. **B)** A representative graph showing NAT10 levels in VSMCs grown on 2, 12 and 72 kPa hydrogels, the dots on the graph represent data points for each repeat of the experiment for all 3 hydrogel stiffnesses. NAT10 has a known molecular weight of 116kDa C) A representative graph showing PDLIM1 levels in VSMCs on 2, 12 and 72 kPa hydrogels. PDLIM1 has a molecular weight of 36kDa. **D)** A representative graph showing ANXa3 levels in VSMCs on 2, 12 and 72 kPa hydrogels. ANXa3 has a molecular weight of 36kDa. **E)** A representative graph showing Chk2 levels in VSMCs on 2, 12 and 72 kPa hydrogels. Ckl2 has a molecular weight of 66kDa. All results were collected from 3 independent repeats (N=3) and a mean was calculated from this and normalised to the control GAPDH. All statistical testing was carried out on the mean data and a one-way ANAOVA test was used.
(All graphs were produced in Biorender.com)

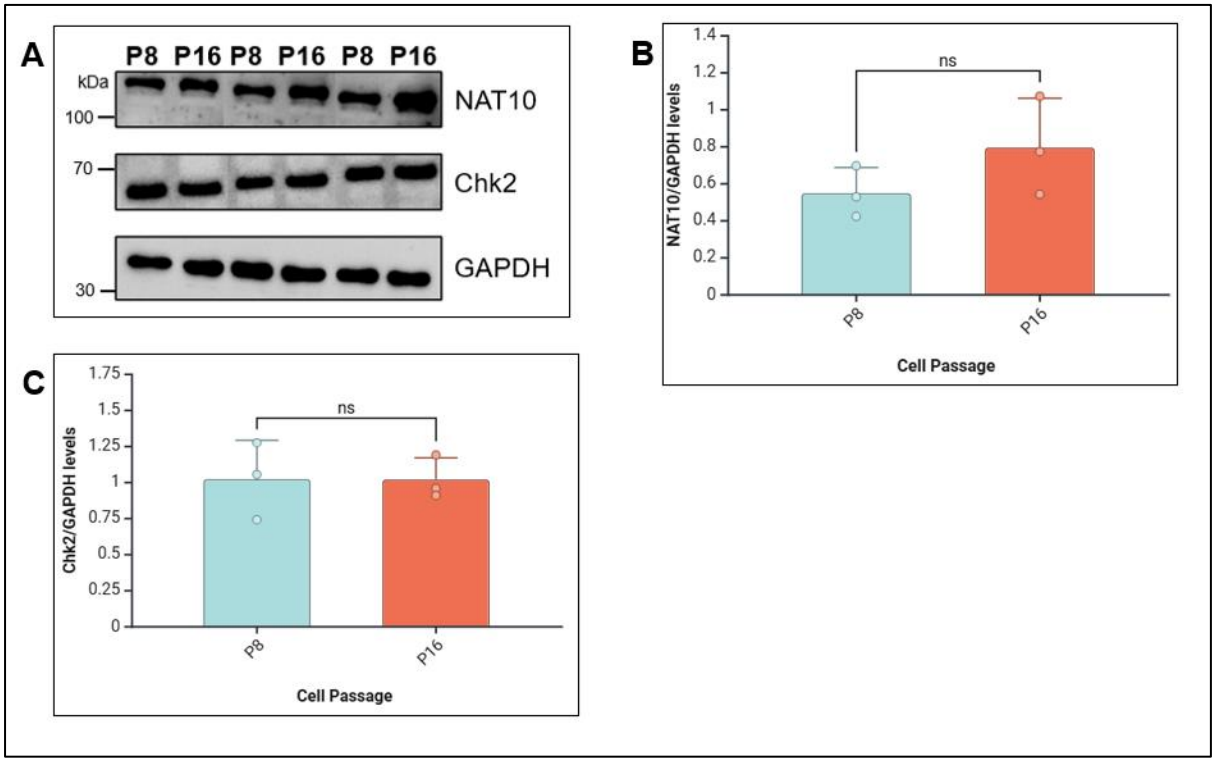

Figure 19. A) Representative western blot of VSMCs collected from passage 8 and 16, probed with NAT10 and Chk2 selected from a list of upregulated genes identified in the mRNAseq data set. **B)** A representative graph showing NAT10 levels in VSMCs from cells at P8 and P16. NAT10 is known to have a molecular weight of 116kDa. **C)** A representative graph showing Chk2 levels in VSMCs from cells at P8 and P16. Chk2 has a molecular weight of 66kDa. All results were collected from 3 independent repeats (N=3) and a mean was calculated from this and normalised to the control GAPDH. All statistical testing was carried out on the mean data and an unpaired two-tailed t-test was used.
(All graphs were produced in Biorender.com)

4. Discussion

In this study, we first investigated how microtubule stability changes with ageing. This was carried out through 3 different experiments: firstly, through testing cells grown on hydrogels. Hydrogels were used to mimic the stiffness of the ECM of the aorta in both healthy cells and aged cells. Additionally, cells were collected at passage 8 and passage 16, this allows a direct comparison of cells from significantly different passage ages.

Upon investigation of this, in the 12 kPa versus the 72 kPa hydrogels, there was no change in levels of acetylated α-tubulin in the aged 72 kPa gels. Moreover, there was no change in levels of acetylated α-tubulin between the younger P8 and the older P16 cell lysates. This suggests that there is no change in α-tubulin acetylation in response to matrix stiffness increases or in cellular ageing. Although it would have been expected for there to be an increase in tubulin acetylation in response to cell age and stiffness changes, the literature surrounding microtubule stability, and the role of tubulin acetylation is contradictory and controversial [98,124]. It would have been expected that because of ECM remodelling induced by age, the aorta becomes stiffer and less pliable. Therefore, in response to increased matrix stiffness, acetylation of α-tubulin would increase to provide increased microtubule stability to compensate for the changes in stiffness. However, this was not found to be true, in response to changes in matrix stiffness or ageing. There was no change in the levels of alpha-tubulin acetylation in cells. This suggests that alpha-tubulin acetylation does not play an important role in cell ageing or matrix stiffness response in VSMCs.

Next, we investigated changes in post-translational modifications of the microtubule stabilising protein Tau during ageing, Tau phosphorylation levels were observed in cells which had undergone a SiRNA FACE1 knockdown. It is also known that as cells age Tau aggregates and can no longer bind to microtubules, Tau proteins are often phosphorylated in their unbound state. It is believed that aggregation of Tau seen in ageing is likely to contribute to an increase in Tau phosphorylation due to the increase in Tau in its unbound state. VSMC dysfunction is known to promote the hyperphosphorylation of Tau. This results in the self-assembly of straight or helical filaments that are involved in Alzheimer's and other Tauopathies [98]. Tau accumulation is also correlated with the loss of contractile phenotype in VSMCs [125]. However, this was not found to be true in this study. Suggesting that the role of Tau is not as important in VSMC ageing as believed and that other factors drive VSMC phenotypic switching. When investigating the impacts of cellular ageing using a FACE1 knockdown, there was no change in Tau phosphorylation in either knockdown.

Furthermore, we investigated changes in phospho-GSK3β levels, GSK3β is a Tau kinase which directly phosphorylates Tau along with a number of other kinases including JNK

and Cdk5. However, GSK3β is also important in regulating notch signalling in VSMCs, GSK3β activates Notch signalling resulting in an increase in proliferation and decrease in apoptosis in VSMCs [126]. Phosphorylation of GSK3β results in a switch to an inactive form which results in reduced Tau phosphorylation but also increased VSMC apoptosis. However, we found that the levels of phospho-GSK3β did not change in mimicked ageing using the FACE1 knockdown experiments. This suggests that the rate of GSK3β phosphorylation is not influenced by matrix stiffness or ageing.

In this study, the Tau and GSK3β experiments were only carried out a single time due to a range of problems that arose during this study. Mainly time restraints and the difficulty of optimising working with Tau antibodies due to their notoriously tricky nature to work properly on western blots. This prevented me from being able to carry out investigating Tau levels on hydrogels for matrix stiffness.

Additionally, the SiFACE1 knockdown proved to be inaccurate and was not working as expected, when probed with pre-lamin A, there was no change in levels in the control compared to the OLIG2 and OLIG4 knockdowns. This is because FACE1 results in an accumulation of pre-lamin A [44] whereas in the control pre-lamin A should be converted to lamin A and therefore levels of pre-lamin A are expected to be lower than in the knockdown. This brought into question the quality and validity of the Si knockdown and it was decided that moving forward in this project, the SiFACE1 would not be used again. Therefore, the results produced by the SiFACE1 knockdown are only preliminary and repeats using newer validated knockdowns would need to be carried out to confirm the results found in this study.

Next, we investigated if both matrix stiffness response and ageing had shared post-translational modifications of histone H3K9. From the surrounding literature, it is known that H3K9 acetylation causes the histone to unwind exposing the chromatin and DNA binding sites and allowing transcription factors to bind [84] inducing cellular responses, resulting in reduced MMP and IL6 expression which are often seen in aged and damaged cells [87].

To investigate stiffness response cells were grown on 2 kPa, 12 kPa and 72 kPa hydrogels. When investigating acetylation levels of H3K9 there was a statistically significant decrease between 2 kPa and 12 kPa, and no change between 2 kPa and 72 kPa, which shows that there is a decrease in acetylation in response to stiffness. This suggests that histone acetylation isn't affected by changes in matrix stiffness. However, when investigating H3K9 acetylation in aged cells using cell lysates collected from passage 8 (young) and passage 16 (old), there was an increase in levels of acetylation in the older passage 16 cells, although the increase was not found to be statistically significant. This suggests that acetylation is increased in response to ageing, this could be a response to cellular changes caused by age

such as matrix remodelling caused by MMPs which H3K9 acetylation is known to reduce. Additionally, levels of H3K9 methylation were also investigated. In response to matrix stiffness increases methylation levels of H3K9 were significantly increased between 2, 12 and 72 kPa, there was also an increase in methylation in the aged passaged 16 cells compared to the passage 8 cells. This shows that methylation is increased in both matrix stiffness response and ageing. We know from Harman et al., that reduction in methylation promotes AP-1 binding and NFκB activation, activating inflammation responses to MMPs and IL6 [96]. The results found in this study suggest that with cell age and matrix stiffness increases, the increase in H3K9 methylation could contribute to the inhibition of AP-1 binding and nuclear factor kappa B (NFκB) activation, resulting in the blocking of inflammation factors, allowing MMPs and IL6 to continue to contribute towards matrix remodelling and vascular dysfunction. Future work could involve developing a way to reduce methylation and increase acetylation of H3K9 to reduce MMP/IL6 expression in aged and diseased cells, through therapeutic targets.

Using mRNAseq data collected from hASMCs identified a host of key genes which were upregulated in response to increased matrix stiffness response. From this list, four genes were chosen and were investigated and validated using western blotting. Firstly, we found that levels of NAT10 increased in response to stiffness increases between 2 kPa, 12 kPa and 72 kPa. This change in NAT10 levels was also seen in cell ageing, there were higher levels of NAT10 in the aged P16s compared to the P8 cells. This suggests that NAT10 levels increase with both cell age and matrix stiffness and is a shared modification, this is because ageing and matrix stiffness are linked, and both increase with time. The results found in this study could be explained by NAT10's role in SASP's [111], as NAT10 was increased in the aged cells and in response to matrix stiffness, which is known to increase with age, the increased NAT10 levels could contribute to micronuclei formation and the downstream release of MMPs and IL6 which contribute to senescence and cell death and the further cellular dysfunction and ECM remodelling. Additionally, Microtubule stability is regulated through tubulin acetylation caused by NAT10, this results in the remodelling of the microtubule network [128]. NAT10 is inhibited by Remodulin and inhibition results in a reduction of genomic instability and delayed senescence in VSMCs [129].

My study is the first to identify changes in protein levels of NAT10, Chk2, ANXa3 and PDLIM1 in VSMCs. However, A previous study by Balmus et al., found that NAT10 levels increased with age induced by Hutchinson-Gilford Progeria Syndrome (HGPS) which prematurely ages cells [130]. Their experiment used cells from mice and compared healthy cells against HGPS cells, they found NAT10 increased in HGPS. They also treated cells with Remodulin which acetylates and inhibits NAT10 function and found NAT10 levels decreased in the HGPS cells but remained the same in the healthy cells. Additionally, they investigated α-tubulin acetylation

and total α-tubulin levels and found no difference in levels between healthy and HGPS-aged cells in both the acetylated and total α-tubulin. However, upon the inhibition of NAT10, there was an increase in levels of acetylated- α-tubulin in HGPS cells. They concluded that NAT10 inhibition resulted in improvements to mice health span in HGPS as it improved cardiac function, fitness and genomic stability.

My study differs from Balmus et al., in that instead of using mouse-derived fibroblast cells, I used human aortic VSMCs and aged the cells through passaging the cells to investigate ageing instead of using HGPS-derived cells. In their study, they used different dilutions of the antibodies used in western blotting compared to my study. Balmus et al., used a 1:400 dilution for Nat10, 1:500 for acetyl- α-tubulin and 1:1000 for α-tubulin. Whereas in my study, I used a 1:1000 dilution for Nat10, acetyl- α-tubulin and total α-tubulin. Additionally, to investigate whether NAT10 level changes are induced by mechanoresponsive young healthy cells were grown on 2, 12 and 72 kPa hydrogels. The data collected in my study revealed that NAT10 levels were significantly increased in stiffness response and in the aged cells. These findings haven't been identified in human aortic VSMCs before and the upregulation of NAT10 levels in aged cells along with acetylated and total α-tubulin levels remaining the same in age correlate with the study by Balmus et al.

Alongside NAT10, Chk2 and ANXa3 are both involved in the DNA damage pathway Chk2 levels were also increased in both the aged P16 cells and in response to matrix stiffness increases. Chk2 is known for inducing cell cycle arrest and apoptosis via DNA damage [110], one method of inducing DNA damage is through the detection of single or double-stranded DNA breaks and through micronuclei extrusions which activate the cGAS-cGAMP-STING pathway stimulating the release of proinflammation factors, including MMPs and IL6 [131]. Due to NAT10's role in increasing micronuclei formation and Chk2's role in micronuclei detection to induce cell death through the cGAS-cGAMP-STING pathway, suggesting there is a link between NAT10 and Chk2. Additionally, ANXa3 contributes to DNA damage through the activation of EGFR-enhanced DNA protein kinases that induce DNA double-stranded breaks resulting in activation of the DDR and resulting in apoptosis [132]. ANXa3 was found to increase with increased matrix stiffness, ANXa3 is known to phosphorylate and activate the JNK signalling pathway [118] resulting in the promotion of VSMC apoptosis and a reduction in proliferation [133]. The increase in ANXa3 levels in response to ECM stiffness increase suggests that ANXa3 may play a role in senescence due to its activation of JNK signalling and the resulting apoptosis and reduction of proliferation caused by it.

Finally, PDLIM1 was also upregulated in response to increased ECM stiffness, this upregulation suggests that in response to arterial stiffening, PDLIM1 promotes the formation

of stress fibres to increase the contractility of VSMCs to recover the loss in compliance of the aorta due to ECM remodelling.

In conclusion, this study has shown that levels of alpha-tubulin acetylation do not change in response to matrix stiffness **(Figure 19 and Figure 20)**, or in aged cells. It shows that alpha-tubulin acetylation is not affected by age and does not play a role in contributing towards or mitigating ageing. It also suggests that microtubule stability is not altered in response to ageing Additionally, Tau phosphorylation is not changed by age. Although, this is only preliminary and impacted by issues with the validity of the SiRNA knockdown used which prevented repeats of this experiment. H3K9 acetylation and methylation were both increased in response to matrix stiffness increases and ageing. Whilst increased acetylation is known to reduce MMP and IL6 activity in cells, methylation is known is increase MMP and IL6 activity through the inhibition of AP-1 binding. Whilst the function of both is known, the interplay between acetylation and methylation and their impact on VSMCs is not yet understood.

The data collected from mRNAseq revealed many genes that are crucial to many biological processes that were upregulated in stiffness response **(Figure 20)**. NAT10 and Chk2 were proven to also be upregulated in ageing as well **(Figure 21)**. NAT10, Chk2 and ANXa3 all promote apoptosis [118] and senescence [110] through MMPs, IL6 or JNK signalling and are all upregulated in matrix stiffness response and cellular ageing. This shows that they directly contribute towards senescence and cell death. PDLIM1 was also upregulated in matrix stiffness response, however, its relationship with VSMCs is very different, it upregulates stress fibre formation [31], suggesting it plays a more regenerative role, in restoring some of the contractile ability of VSMCs to mitigate the loss of aortic compliance in ageing. This experiment is not without its limitations, although western blots and densitometry analysis are good for identifying changes, they cannot quantify these changes. This is because there are many changing factors in western blotting, which can include background levels when imaging, also, primary antibodies can work differently each time they are used which makes western blot results hard to reproduce. Additionally, densitometry is not always suitable for quantifying changes, this is because background levels and “ghost” bands impact the densitometry analysis and provide unrepresentative data. In order to test if the data collected through western blotting is correct and quantifiable, inhibitors of each of the identified genes would have to be used and the effects of this on VSMC mechanoresponsive would need to be identified using confocal microscopy to investigate changes in stiffness response.

Future work could be carried out to target these identified genes and their encoded proteins to inhibit or stimulate their function in cells. NAT10 and Chk2 have been strongly linked to

atherosclerosis, and targeting these proteins and their pathways could serve as a potential therapeutic target for treating atherosclerosis. Additionally, testing these same antibodies in senescent cells, to induce senescence in vitro, oxidative stress could be placed on cells using hydrogen peroxide. Senescent cells could then be lysed and ran out on western blots and probed with the same antibodies identified in the bulk RNA sequence data set. This could be invaluable research as it would allow the comparison of protein level changes between matrix stiffness response, cell age and then cell senescence.

Additionally, by testing the same antibodies and ideas in vivo using animal models such as mice which have similar aortas to humans. Using this model, protein levels can be identified in young and old mice.

Bulk RNA sequencing carried out by the Warren lab using cells grown on 12kPa and 72kPa hydrogels will provide a list of new genes that were upregulated in stiffness response, from these identified genes, related protein levels can be investigated in VSMCs to investigate if the target proteins are increased in stiffness response and age.

Finally, incorporating 2-dimensional gel electrophoresis will allow the identification of the type of modification happening to the target proteins will allow a deeper understanding of what is happening. These gels, first run cell lysate samples by their electrical charge based on pH separating by their isoelectric points. And then a second gel run by molecular weight. This separates proteins out in a way which allows the identification of the type of modification based on the presence of bands or dots.

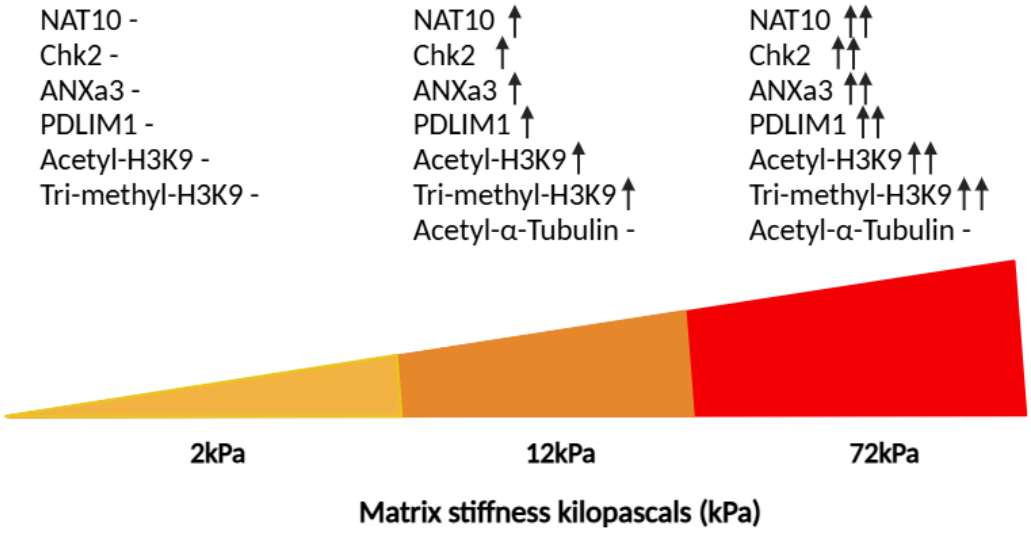

Figure 20.

Overall findings of this study when investigating matrix stiffness response. Protein levels of all investigated proteins increased with matrix stiffness apart from acetylated alpha-tubulin which remained unchanged.

(Figure generated in biorender.com)

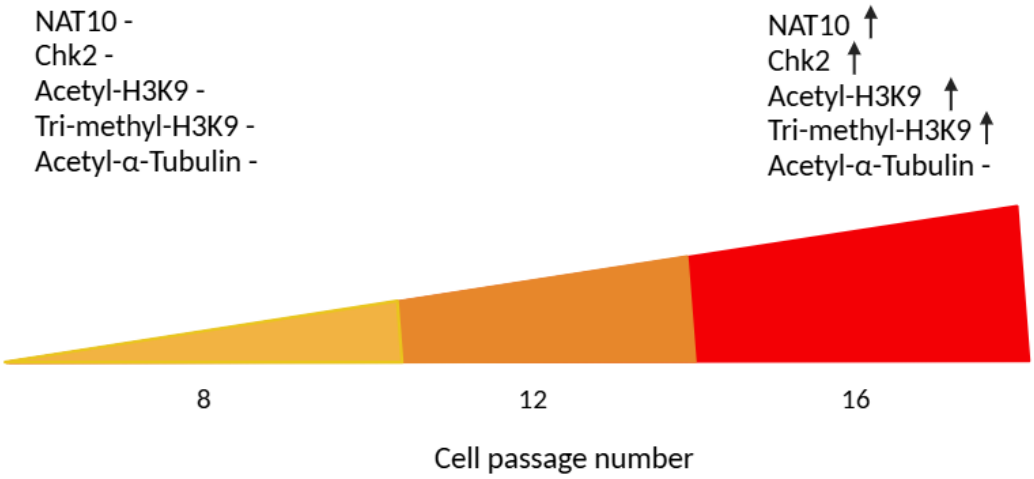

Figure 21.

Overall findings of this study when investigating ageing. Protein levels of all investigated proteins increased with cell age between passage 8 and 16 apart from acetylated alpha-tubulin which remained unchanged.

(Figure generated in biorender.com)

6. Bibliography

1. Ahmed, S. and Warren, D. (2018). Vascular smooth muscle cell contractile function and mechanotransduction. *Vessel plus*. 2(36), p.1-13.
2. Murata, K., Motayama, T. and Kotake, C. (1986). Collagen types in various layers of the human aorta and their changes with the atherosclerotic process. *Atherosclerosis*. 60(3), p.251-262.
3. De Lucio, M., Garcia, M., Garcia J., Rodriguez, L. and Marcos, F. (2021). On the importance of tunica intima in the aging aorta: a three-layered in silico model for computing wall stresses in abdominal aortic aneurysm**s**. *Publication Cover Computer Methods in Biomechanics and Biomedical Engineering*. 24(5), p.467-484.
4. Davies, J., Baksi, J., Francis, D., Hadjiloizou, N., Whinnett, Z., Manisty, C., Aguado-Sierra, J., Foale, R., Malik, I., Tyberg, J., Parker, K., Mayet, J. and Hughes, A. (2010). The arterial reservoir pressure increases with aging and is the major determinant of the aortic augmentation index. *American Journal of Physiology Heart and Circulation Physiology*. 298(2), p.580–586.
5. Steucke, K., Tracy, P., Hald, P., Hall, J., and Alfo, P. (2015). Vascular smooth muscle cell functional contractility depends on extracellular mechanical properties. *Journal of Biomechanics*. 48(12), p.3044–3051.
6. Iddawela, S., Ravendren, A. and Harky, A. (2021). Bio-chemo-mechanics of the thoracic aorta. *Vascular Biology*. 3(1), p.25-33.
7. Lyle, A. and Raaz, Uwe. (2017). Killing Me Unsoftly: Causes and Mechanisms of Arterial Stiffness. *Arteriosclerosis, Thrombosis, and Vascular Biology*. 37(2), p.1-11.
8. Berillis, P. (2013). The Role of Collagen in the Aorta's Structure. *The Open Circulation & Vascular Journal*. 6(1), p.1-8.
9. Singh, C., Wong, C. and Wang, X. (2015). Medical Textiles as Vascular Implants and Their Success to Mimic Natural Arteries. *Journal of Functional Biomaterials*. 6(3), p.500-525.
10. Mohabeer, A., Kroetsch, J., McFadden, M., Khosraviani, N., Broekelmann, T., Hou, G., Zhang, H., Mecham, R., Heximer, S., Bolz, S. and Bendeck, M. (2021). Deletion of type VIII collagen reduces blood pressure, increases carotid artery functional distensibility and promotes elastin deposition. *Matrix Biology Plus*. 12(1), p.1-19.
11. Miekus N., Luise, C., Sippl, W., Baczek, T., Schmelzer, C. and Heinz, A. (2019). MMP-14 degrades tropoelastin and elastin. *Biochimie*. 165(1), p.32-39.
12. Zarkovic, K., Larroque-Cardoso, P., Pucelle, M., Salvayre, R., Waeg, G., Nègre-salvayre, A. and Zarkovic, N. (2015). Elastin aging and lipid oxidation products in human aorta. *Redox Biology*. 4(1), p.109-117.

13. Martin, C., Sun, W., Primiano, C., McKay, R. and Elefteriades, J. (2013). Age-dependent ascending aorta mechanics assessed through multiphase CT. *annals of Biomedical Engineering*. 41(12), p.2565-2574.
14. Collins, J., Munoz, J., Patel, T., Loukas, M. and Tubbs, S. (2014). The Anatomy of the Aging Aorta. *Clinical Anatom*. 27(3), p.463–466
15. Fujimoto, D. (1982). Aging and cross-linking in human aorta. *Biochemical and Biophysical Research Communications*. 109(4), pp.1264-1269.
16. Tsamis , A., Krawiec, J. and Vorp, D. (2013). Elastin and collagen fibre microstructure of the human aorta in ageing and disease: a review. *Journal of The Royal Society Interface*. 10(83), p.1-22.
17. Yamauchi, M. and Sricholpech, M. (2012). Lysine post-translational modifications of collagen. *Essays Biochem*. 52(1), p.113–133
18. Kaya, M., Balasubramanian, V., Patel, A., Ge, Y., and Li, J. (2018). A novel compliance-pressure loop approach to quantify arterial compliance in systole and in diastole. *Computers in Biology and Medicine*. 99(1), p.98-106.
19. Rudijanto, A. (2007). The Role of Vascular Smooth Muscle Cells on The Pathogenesis of Atherosclerosis. *Acta Med Indonesiana - The Indonesian Journal of Internal Medicine*. 39(2), p.86-93.
20. Cao, G., Xuan, X., Hu, J., Zhang, R., Jin, H. and Dong, H. (2022). How vascular smooth muscle cell phenotype switching contributes to vascular disease. *Cell communication and signalling*. 20(180), p.1-22.
21. Chakraborty, R., Chatterjee, P., Dave, J., Ostriker, A., Greif, D., Rzucidlo, E. and Martin, K. (2021). Targeting smooth muscle cell phenotypic switching in vascular disease. *JVS Vasc Sci.*. 2(1), p.79–94.
22. Garoffolo, G., Madonna, R., Caterina, R. and Pesce, M. (2018). Cell based mechanosensing in vascular patho-biology: More than a simple go-with the flow. *Vascular Pharmacology*. 111(1), p.7-14.
23. Johnson, R., Ahmed, S., Solanki, R., Wostear, F., Afewerki, T. and Warren, D. (2022). BS18 Enhanced matrix stiffness prevents vsmc contractility: how calcium signalling and microtubule stability regulate vascular compliance during ageing. *Heart*. 108(1), p.155-155.
24. Afewerki, T., Ahmed, S., and Warren, D. (2019). Emerging regulators of vascular smooth muscle cell migration. *Journal of muscle research and cell motility*, *40*(2), p.185–196
25. Rensen, S., Doevendans, P. and Eys, G. (2007). Regulation and characteristics of vascular smooth muscle cell phenotypic diversity. *Netherlands Heart Journal*. 15(3), p.100-108.

26. Brozovich F. V., Nicholson C. J., Degen C. V., Gao Y. Z., Aggarwal M., Morgan K. G. (2016). Mechanisms of Vascular Smooth Muscle Contraction and the Basis for Pharmacologic Treatment of Smooth Muscle Disorders. Pharmacol. Rev. 68(2), p.476–532.
27. Li, Y., Tai, H., Sladojevic, N., Kim, H. and Liao, J. (2021). Vascular Stiffening Mediated by Rho-Associated Coiled-Coil Containing Kinase Isoforms. *Journal of the American Heart Association*. 10(20), p.1-14.
28. MacDonald. J. and Walsh, M. (2018). Regulation of Smooth Muscle Myosin Light Chain Phosphatase by Multi-site Phosphorylation of the Myosin Targeting Subunit, MYPT1. Cardiovascular & Hematological Disorders-Drug Targets. 18(1), p.4-13.
29. Squire, J. (2019). Special Issue: The Actin-Myosin Interaction in Muscle: Background and Overview. International journal of Molecular Sciences. 20(22), p.1-39.
30. Johnson, R., Solanki, R., Wostear, F., Ahmed, S., Taylor, J., Rees, J., Abel, G., McColl, J., Jørgensen, H., Morris, C., Bidula, S. and Warren, D. (2023). Piezo1-mediated regulation of smooth muscle cell volume in response to enhanced extracellular matrix rigidity. *British Journal of Pharmacology*. 181(11), p.1576-1595.
31. Zhou, J., Fan, X., Cheng, J., Liu, W. and Peng, Y. (2021). PDLIM1: Structure, function and implication in cancer. *Cell Stress*. 5(8), p.119–127.
32. Wanjare, M., Agarwal, N. and Gerecht, S. (2015). Biomechanical strain induces elastin and collagen production in human pluripotent stem cell-derived vascular smooth. *Am J Physiol Cell Physiol.*. 309(4), p.271–281.
33. Chistiakov, D., Orekhov, A. and Bobryshev, Y. (2015). Vascular smooth muscle cell in atherosclerosis. *ATCA PHYSIOLOGICA*. 214(1), p.33-50.
34. Ye, G.,Nesmith, A. and Parker, K. (2014). The role of mechanotransduction on vascular smooth muscle myocytes cytoskeleton and contractile function. *The Anatomical Record*. 297(9), p.1758–1769.
35. Yamashiro, Y. and Yanagisawa, H. (2020). The molecular mechanism of mechanotransduction in vascular homeostasis and disease. *Clinical Science (London)*. 134(17), p.2399–2418.
36. Jiang, Y. and Ji, J. (2018). Understanding lamin proteins and their roles in aging and cardiovascular diseases. *Life Sciences*. 212(1), p.20-29.
37. Monte-Monge, A., de Lara, í., Gonzalo, P., Espinós-Estévez, C., González-Amor, M., Fanjul, V., Gimeno, J., Barriales-Villa, R., Dorado, B. and Andrés, V. (2023). Lamin A/C Ablation Restricted to Vascular Smooth Muscle Cells, Cardiomyocytes, and Cardiac Fibroblasts Causes Cardiac and vascular dysfunction. *International Journal of Molecular Science*. 24(13), p.11172.

38. Donnaloja, F., Carnevali, F., Jacchetti, E. and Raimondi, M. (2020). Lamin A/C Mechanotransduction in Laminopathies. Cells. 9 (5), p.1306-1339.
39. Stroud, M., Banerjee, I., Lowe, J. and Chen, J. (2014). LINC complex proteins in cardiac structure, function, and disease. Circ Res. 114(3), p.538-548.
40. Stierlé V., Couprie J., Ostlund C., Krimm I., Zinn-Justin S., Hossenlopp P., Worman H., Courvalin J. and Duband-Goulet I. (2003). The carboxyl-terminal region common to lamins A and C contains a DNA binding domain. Biochemistry. 42(1), p.4819–4828.
41. Swift, J. and Discher, D. (2014). The nuclear lamina is mechano-responsive to ECM elasticity in mature tissue. Journal of Cell Science. 127(14), p.3005-3015.
42. Petillo, R., D'Ambrosio, P., Torella, A., Taglia, A., Picillo, E., Testori. A,, Ergoli, M., Nigro, G., Piluso, G., Nigro, V. and Politano, L. (2015). Novel mutations in LMNA A/C gene and associated phenotypes. Acta Myologica. 34(3), p.116-119.
43. Storch, K. and Cordes, N. (2012). Focal Adhesion-Chromatin Linkage Controls Tumor Cell Resistance to Radio- and Chemotherapy. Chemotherapy Research and Practice. 1(4), p.1-11.
44. Corrigan, D., Kuszczak, D., Rusinol, A., Thewke, D., Hrycyna, C., Michaelis, S. and Sinensky, M. (2005). Prelamin A endoproteolytic processing in vitro by recombinant Zmpste24. Biochemical Journal. 387(1), p.129-138.
45. Warren, D. and Shanahan, C. (2011). Defective DNA-damage repair induced by nuclear lamina dysfunction is a key mediator of smooth muscle cell aging. Biochemical Society Transactions. 39(6), p.1780-1785,
46. Bosco, E., Mulloy, J. and Zheng, Y. (2009). Rac1 GTPase: A “Rac” of All Trades. *Cell Mol Life Sci.*. 66(3), p.370–374.
47. Kim, H., Appel, S., Vetterkind, S., Gangopadhyay, S. and Morgan, K. (2008). Smooth muscle signalling pathways in health and disease. *Journal of Cellular Molecular Medicine*. 12(6), p.2165–2180.
48. Liu, S. and Lin, Z. (2022). Vascular Smooth Muscle Cells Mechanosensitive Regulators and Vascular Remodeling. *Journal of Vascular Research*. 59(2), p.90–113.
49. Zhang, J., Zhou, Y., Tang, P., Cheng, A., Yu, J., To, K. and Kang, W. (2020). Mechanotransduction and Cytoskeleton Remodeling Shaping YAP1 in Gastric Tumorigenesis. *International Journal of Molecular Science*. 20(7), p.1576.
50. Li, R. and Huang, W. (2023). Yes-Associated Protein and Transcriptional Coactivator with PDZ-Binding Motif in Cardiovascular Diseases. *Internation Journal of Molecular Sciences*. 24(2), p.16-66.

51. Zhang, S., Zhang, Q., Lu, Y., Chen, J., Liu, J., Li, Z. and Xie, Z. (2024). Roles of Integrin in Cardiovascular Diseases: From Basic Research to Clinical Implications. International Journal of Molecular Sciences. 25(7), p.1-29.

52. Chen, X., Lin, J., Hu, T., Ren, Z., Li, L., Hameed, I., Zhang, X., Men, C., Guo, Y., Xu, D. and Zhan, Y. (2018). Galectin-3 exacerbates ox-LDL-mediated endothelial injury by inducing inflammation via integrin β1-RhoA-JNK signaling activation. Journal of Cell Physiology. 234(7), p10990-11000.

53. Chiang, H., Chu, P., Chen, S. and Lee, T. (2022). MFG-E8 promotes osteogenic transdifferentiation of smooth muscle cells and vascular calcification by regulating TGF-β1 signaling. Communications Biology. 5(364), p.1-13.

54. Govatati, S., Pichavaram, P., Kumar, R. and Rao, G. (2023). Blockade of CD47 function attenuates restenosis by promoting smooth muscle cell efferocytosis and inhibiting their migration and proliferation. Journal of Biological Chemistry. 299(4), p.1-18.
55. Philippova M, Bochkov V, Stambolsky D, Tkachuk V, Resink T. (1998) T-cadherin and signal-transducing molecules co-localize in caveolin-rich membrane domains of vascular smooth muscle cells. *Federation of European Biochemical Societies Letters.* 429(1), p.207–210.
56. Cao, R., Tian, H., Tian, Y. and Fu, X. (2023). A Hierarchical Mechanotransduction System: From Macro to Micro. Advanced Science. 11(11), p.1-32.
57. Dominguez, R. and Holmes, K. (2011). Actin Structure and Function. *Annual Review of Biophysics*. 40(1), p.169–186.
58. Shi, Y. and Massagué, J. (2003). Mechanisms of TGF-β Signaling from Cell Membrane to the Nucleus. Cell. 113(6), p.685-700.
59. Burridge, K., Molony, L. and Kelly, T. (1987). Adhesion Plaques: Sites of Transmembrane Interaction Between the Extracellular Matrix and the Actin Cytoskeleton. *Journal of Cell Science*. 8(1), p.211–219.
60. Fels, B. and Kusche-Vihrog, K. (2020). It takes more than two to tango: mechanosignaling of the endothelial surface. *European journal of physiology*. 472(1), p.419–433.
61. Davis, M., Earley, S., Li, Y. and Chien, S. (2023). Vascular mechanotransduction. *Physiological Reviews*. 103(2), p.1247–1421.
62. Williams, B. (1998). Mechanical influences on vascular smooth muscle cell function. *Journal of hypertension*. 16(12), p.1921-1929.

63. Liu, Z., Wang, Q. Zhang, J. Qi, S., Duan, Y. and Li, C. (2023).The Mechanotransduction Signaling Pathways in the Regulation of Osteogenesis. International Journal of Molecular Sciences. 24(18), p.1-23.
64. Osol, G. (1995). Mechanotransduction by Vascular Smooth Muscle. *Journal of vascular research*. 32(5), p.275–292.
65. Ridone, P., Vassalli, M. and Martina, B. (2019). Piezo1 mechanosensitive channels: what are they and why are they important. *Biophysical Reviews*. 11(5), p.795-805.
66. Tempest, R., Guarnerio, S., Maani, R., Cooper, J. and Peake, N. (2021). The Biological and Biomechanical Role of Transglutaminase-2 in the Tumour Microenvironment. *Cancers (Basel)*. 13(11), p.2788-2816.
67. Johnston, C. (1990). Biochemistry and Pharmacology of the Renin-Angiotensin System. *Drugs*. Volume 39(1), p.21–31.
68. Berk, B. and Corson, M. (1997). Angiotensin II signal transduction in vascular smooth muscle: role of tyrosine kinases. *Circulation Research*. 80(5), pp.607-616.
69. Reid, D. and Nicchitta, C. (2015). Diversity and selectivity in mRNA translocation on the endoplasmic reticulum. Nature Reviews Molecular Cell Biology. 16(1), p.221-231.
70. Gregory, B., Rahman, N., Bommakanti, A., Shamsuzzaman, M., Thapa, M., Lescure, A., Zengel, J. and Lindahl, L. (2019). The small and large ribosomal subunits depend on each other for stability and accumulation. Life Science Alliance. 5(2), p.1-18.
71. Balchin, D., Hayer-Hartl, M. and Hartl, U. (2016). In vivo aspects of protein folding and quality control. Science. 353(6294), p.42-55.
72. Zimmerman, R., Eyrisch, S., Ahmad, M. and Helms, V. (2011). Protein translocation across the ER membrane. Biochimica et Biophysica Acta (BBA) – Biomembranes. 1808(3), p.912-924.
73. Ma, Y. and Hendershot, L. (2004). ER chaperone functions during normal and stress conditions. Journal of Chemical Neuroanatomy. 28(1), p.51-65.
74. Schröder, M. and Kaufman, R. (2005). ER stress and the unfolded protein response. Mutation research/fundamental and molecular mechanisms of mutagenesis. 569(1), p.29-63.
75. Potelle, S., Klein, A. and Foulquier, F. (2015). Golgi post-translational modifications and associated diseases. Journal of Inherited Metabolic Disease. 38(1), p.741-751.
76. Reily, C., Stewart, T., Renfrow, M. and Novak, J. (2019). Glycosylation in health and disease. Nature Reviews Nephrology. 15(1), p.346-366.
77. Yang, X., Yu, W., Shi, L., Yang, J., Yao, Z. and Shang, Y. (2011). HAT4, a Golgi Apparatus-Anchored B-Type Histone Acetyltransferase, Acetylates Free Histone H4 and Facilitates Chromatin Assembly. Molecular Cell. 44(1), p.39-50.

78. Sun, J., Tai, S., Tang, L., Yang, H., Chen, M., Xiao, Y., Li, X., Zhu, Z., and Zhou, S. (2021). Acetylation Modification During Autophagy and Vascular Aging. Frontiers of Physiology. 12 (1), p.1-10.
79. Murn, J. and Shi, Y. (2017). The winding path of protein methylation research: milestones and new frontiers. Nature Reviews Molecular Cell Biology. 18(1), p.517-527.
80. Zhuang, J. Luan, P., Li, H., Wan=ng, K., Zhang, P., Xu, Y. and Peng, W. (2016). The Yin–Yang Dynamics of DNA Methylation Is the Key Regulator for Smooth Muscle Cell Phenotype Switch and Vascular Remodelling. Arteriosclerosis, Thrombosis and Vascular Biology. 37(1), p.84-97.
81. Lopez, S., Segal, D. and LaSalle, J. (2019). UBE3A: An E3 Ubiquitin Ligase With Genome-Wide Impact in Neurodevelopmental Disease. Frontiers of Molecular Neuroscience. 11(1), p.1-8.
82. Brinkmann, K., Schell, M., Hoppe, T. Kashkar, H. (2015). Regulation of the DNA damage response by ubiquitin conjugation. Frontiers in Genetics. 6(1), p.1-15.
83. Vlad, D., Dumitrascu, D. and Dumitrascu, A. (2023). Golgi's Role in the Development of Possible New Therapies in Cancer. Cells. 12(11), p.1499-1511.
84. Miller, J. and Grant, P. (2013). The Role of DNA Methylation and Histone Modifications in Transcriptional Regulation in Humans. *Subcell Biochem*. 61(1), p.289–317.
85. Greißel, A., Culmes, M., Burgkart R., Zimmermann, A., Eckstein, H., Zernecke, A. and Pelisek, J.(2016). Histone acetylation and methylation significantly change with severity of atherosclerosis in human carotid plaques. *Cardiovascular Pathology*. 25(1), p.79–86.
86. Stoll, S., Wang, C. and Qiu, H. (2018). DNA Methylation and Histone Modification in Hypertension. *International Journal of Molecular Science*. 19(4), p.1174-1191.
87. Harman, J., ,Dobnikar, L., Chappell, J., Stokell, B., Dably, A., Foote, K., Finigan, A., Freire-pritchett, P., Taylor, A., Worssam, M., Madsen, R., Loche, E., Uryga, A., Bennett, M. and Jørgensen, H. (2019). Epigenetic Regulation of Vascular Smooth Muscle Cells by Histone H3 Lysine 9 Dimethylation Attenuates Target Gene-Induction by Inflammatory Signalling. *Arterioscler Thromb Vasc Biol*. 39(11), p.2289–2302.
88. Binarová, P. and Tuszynski, J. (2019). Cells. *Tubulin: Structure, Functions and Roles in Disease*. 8(10), p.1294
89. Michaels, T., Feng, S., Liang, H. and Mahadevan, L. (2020). Mechanics and kinetics of dynamic instability. *eLife*. 9(1), p.1-29.
90. Caporizzo, M. and Prosser, B. (2022). The microtubule cytoskeleton in cardiac mechanics and heart failure. *Nature Reviews Cardiology*. 19(6), p.364–378.

91. Janke, C. and Magiera, M. (2020). The tubulin code and its role in controlling microtubule properties and functions. *Nature Reviews Molecular Cell Biology*. 21(1), p.307–326.
92. Zhang, Y., Li, N., Caron, C., Matthias, G., Hess, D., Khochbin, S. and Matthias, P. (2003). HDAC-6 interacts with and deacetylates tubulin and microtubules in vivo. *The EMBO Journal*. 22(1), p.1168 - 1179.
93. Takemura, R., Okabe, S., Umeyama, T., Kanai, Y., Cowan, N. and Hirokawa, N. (1992). Increased microtubule stability and alpha tubulin acetylation in cells transfected with microtubule-associated proteins. *Journal of Cell Science*. 103(4), p.953–964.
94. Mozzicato, A., Bastrup, J., Sanchez-Alonso, J., van der Horst, J., Gorelik, J., Hägglund, P. and Jepps, T. (2024). Mesenteric artery smooth muscle cells from hypertensive rats have increased microtubule acetylation. *Biochemical Journal*. 481(5), p.387–403.
95. Cueva J., ,Hsin, J., Huang, K. and Goodman, M. (2012). Posttranslational Acetylation of a-Tubulin Constrains Protofilament Number in Native Microtubules. *Current Biology*. 22(1), p.1066–1074.
96. Bär, J., Popp, Y., Bucher, M. and Mikhaylova, M. (2022). Direct and indirect effects of tubulin post-translational modifications on microtubule stability: Insights and regulation. *Biochimica et Biophysica Acta (BBA) - Molecular Cell Research*. 1869(6), p.1-11.
97. Seto, E. and Yoshida, M. (2014). Erasers of Histone Acetylation: The Histone Deacetylase Enzymes. *Cold Spring Harbor Perspectives in Biology*. 6(4), p.a018713.
98. Eshun-Wilson, L., Zhang, R., Portran D., Nachury M., Toso D., Löhr T., Vendruscolo, M., Bonomi, M., Fraser J. and Nogales, E. (2019). Effects ofα-tubulin acetylation on microtubulestructure and stability. *Proceedings of the National Academy of Sciences*. 116(21), p.10366 - 10371.
99. Habibian, J. and Ferguson, B. (2019). The Crosstalk between Acetylation and Phosphorylation: Emerging New Roles for HDAC Inhibitors in the Heart. *International Journal of Molecular Science*. 20(1), p.102.
100. Mukaetova-Ladinska, E., Abdel-All, Z., Mugica, E., Li, M., Craggs, L., Oakley, A., Honer, W. and Kalaria, R. (2015).Tau Proteins in the Temporal and Frontal Cortices in Patients With Vascular Dementia. *Journal of Neuropathology & Experimental Neurology*, 74(2), p.148–157
101. Aguilar-Pineda, J., Karin J. Vera-Lopez, K., Shrivastava, P., Nieto-Montesinos, R., Chávez-Fumagalli, M., Del-Carpio, G., Gomez Valdez, B., Miller, C., Malhotra, R., Mark E. Lindsay, M. and Lino Cardenas, C. (2021). Vascular smooth muscle cell

dysfunction contribute to neuroinflammation and Tau hyperphosphorylation in Alzheimer disease. *iScience*. 24(1), p.1-21.

102. Ho Lee, T , Pastorino, L and Ping Lu, K. (2011). Peptidyl-prolyl cis–trans isomerase Pin1 in ageing, cancer and Alzheimer disease. *Expert Reviews in Molecular Medicine*. 13(1), p.1-26.

103. Li, C., Wang, Y., Yan, X., Guo, Z. and Yang, Y. (2021). Pathological changes in neurovascular units: Lessons from cases of vascular dementia. *CNS Neuroscience and Therapeutics*. 21(1), p.17-25.

104. Wagner, U., Utton, M., Gallo, J. and Miller, C. (1996). Cellular phosphorylation of tau by GSK-3β influences tau binding to microtubules and microtubule organisation. *Journal of Cell Science*. 109(6), p.1537–1543.

105. Plattner, F., Angelo, M. and Giese, P. (2006). The Roles of Cyclin-dependent Kinase 5 and Glycogen Synthase Kinase 3 in Tau Hyperphosphorylation. *Mechanisms of Signal Transduction*. 281(35), p.25-45.

106. Hussong, S., Banh, A., Van Skike, C., Dorigatti, A., Hernandez, S., Hart, M., Ferran, B., Makhlouf, H., Gaczynska, M., Osmulski, P., McAkken, S., Dineley, K., Ungvari, Z., Perez, V., Kayed, R. and Galvan, V. (2023). Soluble pathogenic tau enters brain vascular endothelial cells and drives cellular senescence and brain microvascular dysfunction in a mouse model of tauopathy. *Nature Communications*. 14(2367), p.1-16.

107. Stewart, D. (2007). Mechanisms of resistance to cisplatin and carboplatin. *Critical reviews in oncology/hematology*. 63(1), p.12–31.

108. Ahn, J., Urist, M. and Prive, C. (2004). The Chk2 protein kinase. *DNA Repair*. 3(8), p.1039-1047.

109. Warren, D., Tajsic, T., Porter, L., Minaisah, R., Cobb, A., Jacob, A., Rajgor, D., Zhang, Q. and Shanahan, C. (2015). Nesprin-2-dependent ERK1/2 compartmentalisation regulates the DNA damage response in vascular smooth muscle cell ageing. *Cell Death Differ*. 22(9), p.1540–1550.

110. Kumari, R. and Jat, P. (2021). Mechanisms of Cellular Senescence: Cell Cycle Arrest and Senescence Associated Secretory Phenotype. *Frontiers in Cell and Developmental Biology*. 9(1), p.1-24

111. Cao, Y., Yao, M., Wu, Y., Ma, N., Liu, H. and Zhang, B. (2020). N-Acetyltransferase 10 Promotes Micronuclei Formation to Activate the Senescence-Associated Secretory Phenotype Machinery in Colorectal Cancer Cells . *Translational Oncology*. 13(8), p.1-10.

112. Khavinson, V., Linkova, N., Dyatlova, A. and Kantemirova, R. (2023). Senescence-Associated Secretory Phenotype of Cardiovascular System Cells and Inflammaging: Perspectives of Peptide Regulation. *Cells*. 12(1), p.106-128
113. Gray, K., Sheetal, K., Figg, N., Harrison, J., Baker, L., Littlewood, T. and Bennett, M. (2014). Effects of DNA Damage in Smooth Muscle Cells in Atherosclerosis. *Circulation Research*. 116(5), p.816-826.
114. Nikfarjam, S. and Singh, K. (2023). DNA damage response signaling: A common link between cancer and cardiovascular diseases. *Cancer Medicine*. 12(4), p.4380–4404.
115. Rass, E., Willaume, S. and Bertrand, P. (2022). 53BP1: Keeping It under Control, Even at a Distance from DNA Damage. *Genes*. 13(12), p.2390-2411.
116. Tong, M., Fung T.M., Luk S.T., Ng K.Y., Lee T.K., Lin C.H., Yam J.W., Chan K.W., Ng F., Zheng B.J. (2015). ANXA3/JNK Signaling Promotes Self-Renewal and Tumor Growth, and Its Blockade Provides a Therapeutic Target for Hepatocellular Carcinoma. *Stem Cell Reports.* 5(1), p.45–59
117. Wang, Y., Chun Wang, C., Yang, Q., and Cheng, Y. (2019). ANXA3 Silencing Ameliorates Intracranial Aneurysm via Inhibition of the JNK Signaling Pathway. *Molecular Therapy - Nucleic Acids.*. 6(17), p.540–550.
118. Dhanasekaran, D. and Reddy, E. (2017). JNK-signaling: A multiplexing hub in programmed cell death. Genes and Cancer. 9(9-10), p.682-694.
119. Ponticos, M., Partridge, T., Black, C., Abraham, D. and Bou-Gharious, G. (2004). Regulation of collagen type I in vascular smooth muscle cells by competition between Nkx2.5 and deltaEF1/ZEB1. Molecular Cell Biology. 24(14), p.6151-6161.
120. Kandow, C., Georges, P., Janmey, P. and Beningo, K. (2007). Polyacrylamide Hydrogels for Cell Mechanics: Steps Toward Optimization and Alternative Uses. Methods in Cell Biology. 83(1), p.29-46.
121. Minaisah, R., Cox, S. and Warren, D. (2016). The Use of Polyacrylamide Hydrogels to Study the Effects of Matrix Stiffness on Nuclear Envelope Properties. Methods in Molecular Biology. 14(11), p.233-239.
122. Johnson, R., Wostear, F., Solanki, R., Steward, O., Bradford, A., Morris, C., Bidula, S. and Warren, D. (2024). A microtubule stability switch alters isolated vascular smooth muscle Ca2+ flux in response to matrix rigidity. Journal of Cell Science. 137(21), p.1-12.
123. Yu, C., Xu, T., Assoian, R. and Rader, D. (2018). Mining the stiffness-sensitive transcriptome in human vascular smooth muscle cells identifies long non-coding RNA stiffness regulators. Atherlosclerosis and Thrombosis Vascular Biology. 38(1), p.164-173.

124. Janke, C. and Montagnac, G. (2017) Causes and Consequences of Microtubule Acetylation. Current Biology. 27(23), p,1287-1292.
125. Hayes, G., Pinto, J., Sparks, S., Wang, C., Suri, S. and Bulte, D. (2022). Vascular smooth muscle cell dysfunction in neurodegeneration. *Frontiers of Neuroscience*. 16(1), p.1-22.
126. Guha, S., Cullen, J., Morrow, D., Colombo, A., Lally, C., Walls, D., Redmond, E. and Cahill, P. (2011). Glycogen synthase kinase 3 beta positively regulates Notch signaling in vascular smooth muscle cells: role in cell proliferation and survival. *Basic Res Cardiol.*. 106(5), p.773–785.
127. Cao, Y., Yao, M., Wu, Y., Ma, N., Liu, H. and Zhang, B. (2020). N-Acetyltransferase 10 Promotes Micronuclei Formation to Activate the Senescence-Associated Secretory Phenotype Machinery in Colorectal Cancer Cells . *Translational Oncology*. 13(8), p.1-10.
128. Ahmed, S. (2021). The effect of matrix stiffness on vascular smooth muscle cell contractility[Doctoral dissertation, University of East Anglia]. UEA Digital Repository https://ueaeprints.uea.ac.uk/id/eprint/84336/1/2021AhmedSPhD.pdf
129. Cobb, A., Delphine Larrieu, D., Warren, D., Liu, Y., Srivastava, S., Smith, A., Bowater, R., Jackson, S. and Shanahan, C. (2016). Prelamin A impairs 53BP1 nuclear entry by mislocalizing NUP153 and disrupting the Ran gradient. *aging cell*. 15(6), p.1039-1050.
130. Balmus, G., Larrieu, G., Barros, A., Collins, C., Abrudan, M., Demir, M., Geisler, N., Lelliott, White, J., Karp, N., Atkinson, J., Kirton, A., Jacobsen, M., Clift, M., Rodriguez, R. Sanger Mouse Genetics Project, Adams, D. and Jackson, S. (2018). Targeting of NAT10 enhances healthspan in a mouse model of human accelerated aging syndrome. Nature Communications. 9 (1700), p.1-14
131. Wang, L., Yang, L., Wang, C., Zhao, W., Ju, Z., Zhang, W., Shen, J., Peng, Y., An, C., Luu, Y., Song, S., Yap, T., Ajani, J., Mills, G., Shen, X. and Peng, G. (2020). Inhibition of the ATM/Chk2 axis promotes cGAS/STING signaling in ARID1A-deficient tumors. Journal of clinical investigation. 130(11)5951-5966.
132. Yang, L., Lu, P., Yang, X., Li, K., Chen, X., Zhou, Y. and Qu, S. (2022). Downregulation of annexin A3 promotes ionizing radiation-induced EGFR activation and nuclear translocation and confers radioresistance in nasopharyngeal carcinoma. (Experimental Cell Research). 418 (2), p.1-14.
133. Picco, V. and Pagès, G. (2013). Linking JNK Activity to the DNA Damage Response. *Genes & Cancer*. 4(9), p.360–368.